

Article

A Quasi-3D Refined Theory for the Vibration of Functionally Graded Plates Resting on Visco-Winkler-Pasternak Foundations

Mashhour A. Alazwari ¹ and Ashraf M. Zenkour ^{2,*}

¹ Mechanical Engineering Department, Faculty of Engineering, King Abdulaziz University, Jeddah 21589, Saudi Arabia; maalazwari@kau.edu.sa

² Department of Mathematics, Faculty of Science, King Abdulaziz University, Jeddah 21589, Saudi Arabia

* Correspondence: zenkour@kau.edu.sa

Abstract: This article establishes the vibrational behavior of functionally graded plates embedded in a viscoelastic medium. The quasi-3D elasticity equations are used for this purpose. The three-parameter Visco-Winkler-Pasternak model is employed to give the interaction between the viscoelastic foundation and the presented plate. Hamilton's principle is applied to derive the governing dynamic equations. Many validation examples are presented. Additional benchmark results are tabulated for future comparisons. The effects of various parameters like geometrical, material properties, and viscoelastic foundations on the vibrational frequencies of homogeneous and functionally graded plates are investigated. The frequencies increase as all parameters increase except the functionally graded power-law index for which its increase causes a decrease in the frequency value.

Keywords: quasi-3D theory; eigenfrequencies; functionally graded plates; Visco-Winkler-Pasternak foundation



Citation: Alazwari, M.A.; Zenkour, A.M. A Quasi-3D Refined Theory for the Vibration of Functionally Graded Plates Resting on Visco-Winkler-Pasternak Foundations. *Mathematics* **2022**, *10*, 716. <https://doi.org/10.3390/math10050716>

Academic Editors: Jan Awrejcewicz and Ali Farajpour

Received: 16 December 2021

Accepted: 21 February 2022

Published: 24 February 2022

Publisher's Note: MDPI stays neutral with regard to jurisdictional claims in published maps and institutional affiliations.



Copyright: © 2022 by the authors. Licensee MDPI, Basel, Switzerland. This article is an open access article distributed under the terms and conditions of the Creative Commons Attribution (CC BY) license (<https://creativecommons.org/licenses/by/4.0/>).

1. Introduction

Functionally graded materials (FGMs), which were proposed by Koizumi [1,2], are widely used in many real-life engineering applications due to their distinct properties which cannot be achieved using traditional materials such as their capability to resist high temperature, high strength, mechanical, and chemical properties. The FGMs are produced by mixing ceramics and metals in which the ceramics and metals enhance the thermal properties and mechanical properties, respectively. Therefore, FGMs become favorable materials for designers in many applications such as aerospace, nuclear, marine, and lightweight structures.

Several structural applications use plates resting on elastic foundations and a lot of research has been conducted to investigate the vibration behavior of FGMs' plates supported by elastic foundations. Here, we restrict our attention to the vibration analyses of different structures that rest on elastic foundations. The most famous model of the elastic foundations is known as the Winkler-Pasternak model or, for simplicity, Pasternak's foundation model. It contains, of course, two parameters, the transverse stiffness coefficient of Winkler and the shear stiffness coefficient of Pasternak. Hosseini-Hashemi et al. [3] presented an analytical solution for the free vibrational analyses of FG rectangular plates resting on Winkler or Pasternak elastic foundations using the first-order shear deformation plate theory (FSDT).

A layerwise finite element formulation was introduced by Pandey and Pradyumna [4] for the free vibration analysis of FG sandwich plates with a nonlinear variation of the temperature through the thickness. Zenkour [5] presented the free vibration of a microbeam resting on Pasternak's foundation via the Green-Naghdi thermoelasticity theory without energy dissipation. The neutral surface concept using the higher-order shear deformation theory (HSDT) was used by Benferhat et al. [6] to investigate the free vibration response

of FGMs plates resting on elastic foundations. Zaoui et al. [7] used the quasi-3D hybrid-type HSDT to study the free vibration of FG plates resting on Pasternak's foundation. Zenkour and Radwan [8] presented the free vibrational analysis of multilayered composite and softcore sandwich plates resting on Winkler-Pasternak foundations. Wang et al. [9] analyzed the thermal vibration of FG graphene platelets reinforced composite annular plate supported by an elastic foundation. Sobhy and Zenkour [10] discussed the vibration of FG graphene, platelet-reinforced, composite, doubly-curved, shallow shells resting on elastic foundations.

The HSDT and the two parameters, Pasternak and Winkler, as the elastic foundation were used by Kumar et al. [11] to study the free vibration of tapered rectangular FG plates. Liu et al. [12] used the FSDT and the multi-segment partition technique for the dynamic analysis of FG plates reinforced with graphene platelets resting on the two-parameter elastic foundation (Pasternak and Winkler). Arefi et al. [13] presented the size-dependent free vibration of a three-layered exponentially graded (EG) nano-/micro-plate with piezomagnetic face sheets resting on Pasternak's foundation via MCST. Furthermore, the two-parameter elastic foundation model was utilized by Tran et al. [14] to investigate the vibration response of FG plates resting on an elastic foundation in a thermal environment. Li et al. [15,16] presented a new semi-analytical method to analyze the free vibration of uniform, stepped, and porous FG cylindrical shells under arbitrary boundary conditions. Radaković et al. [17] presented a mathematical model to discuss the thermal buckling and free vibration of a functionally graded plate that includes interaction with an elastic foundation. Li et al. [18] discussed the vibration analysis of rotating, functionally graded, nano-annular plates in a thermal environment. The edge-based smoothed, finite element method and a mixed interpolation of tensorial components were used by Nguyen et al. [19] to study the free vibration of FG porous plates resting on a two-parameter elastic foundation. Tran et al. [20] used a nonlocal theory based upon four unknowns to complete the analysis of FG porous nanoshells resting on an elastic foundation. Recently, Zenkour and El-Shahrany [21] presented the forced vibration of a magnetoelastic, laminated, composite beam resting on Pasternak's foundation.

If we add the effect of the damping coefficient to the above two-parameter elastic model, we can get the third viscoelastic foundation model. Several publications in the literature are made according to the inclusion of the third parameter to discuss the vibrational problems of structures resting on the viscoelastic foundation [22–26]. The additional elastic foundation model is denoted by Kerr's foundation model. A lot of articles are concerned with the force or the control of the hygrothermal vibration of sinusoidal FG nanobeams or viscoelastic magnetostrictive sandwich plates resting on a hybrid of Kerr's foundation [27,28].

This paper, for the first time, uses the Visco-Winkler-Pasternak elastic foundation model in conjunction with a quasi-3D refined theory to study the vibration response of FG plates. The analytical solutions for the natural vibration analysis of FG plates are developed on the assumption that transverse shear displacements vary as a hyperbolic function through the thickness of the plate. In addition, the transverse normal strain is taken into consideration. Based on the present theory, comprehensive results of non-dimensional frequencies of homogeneous and FG plates with and without the inclusion of the three-parameter viscoelastic foundations are tabulated for future comparisons. Then fundamental/natural frequencies are found by solving the eigenvalue problem. To verify the accuracy of the present theory, many numerical examples are solved and compared with other published solutions in the literature. In addition to the two-parameter elastic foundation, the inclusion of a third damping parameter is also investigated.

2. Basic Equations

2.1. An FG Plate Structure

A functionally graded rectangular plate resting on a three-parameter elastic foundation and bounded by the coordinate planes $x = 0$, a , $y = 0$, b , and $z = -h/2$, $h/2$, as shown in Figure 1, is considered. The Cartesian coordinates x , y , z are chosen such as z is placed on

the middle plane of the FG plate. The FG plate is made from metal (Aluminum-Al) and ceramic (Alumina-Al₂O₃ or Zirconia-ZrO₂) with the properties established in Section 3. The bottom surface of the FG plate is metal-rich, and the top surface is ceramic-rich while the middle is a mixture of both, which is varied using the following power-law function:

$$P(z) = (P_c - P_m) \left(\frac{z}{h} + \frac{1}{2} \right)^p + P_m, \tag{1}$$

where the subscripts *m* and *c* denote metal and ceramic material properties, respectively, and *p* is the gradient index that controls the smooth distribution of material through the thickness of the FG plate and *z* is the distance from the neutral plane of the FG plate.

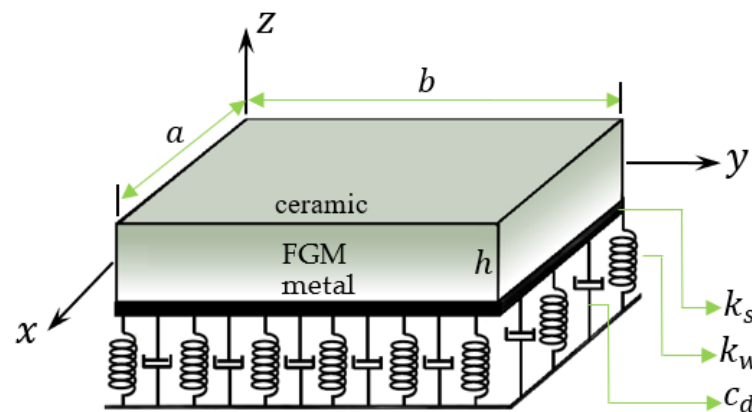


Figure 1. The schematic diagram for the geometry of the FG plate resting on a Visco-Winkler-Pasternak foundation.

2.2. A Quasi 3-D Higher-Order Plate Theory

Let *v_x(x, y, z; t)*, *v_y(x, y, z; t)*, and *v_z(x, y, z; t)* denote the dynamic displacement components of a material point located at (*x, y, z*) and time *t* in the *x*, *y*, and *z* directions, respectively. The in-plane displacements and transverse displacement are assumed according to the following refined quasi-3D plate theory:

$$\left. \begin{aligned} v_\alpha &= u_\alpha - zu_{z,\alpha} + f(z)\phi_\alpha, \\ v_z &= u_z + g(z)\phi_z, \end{aligned} \right\} \alpha = x, y \tag{2}$$

where the above displacements contain six unknowns *u_α*, *w*, and *φ_j* as functions on (*x, y, t*). The effects due to transverse shear strain and normal deformations are both included. The function *f(z)* should be an odd function of *z* while *g(z)* should be an even function. That is

$$f(z) = h \sinh\left(\frac{z}{h}\right) - \frac{4z^3}{3h^2} \cosh\left(\frac{1}{2}\right), \quad g(z) = f'(z), \quad ()' = \frac{d()}{dz}. \tag{3}$$

No transversal shear correction factors are needed for the present model because a correct representation of the transversal shearing strain is given. In the displacement field in Equation (2), the strains are given by

$$\left\{ \begin{aligned} \varepsilon_\alpha \\ \gamma_{xy} \end{aligned} \right\} = \left\{ \begin{aligned} \varepsilon_\alpha^0 \\ \gamma_{xy}^0 \end{aligned} \right\} + z \left\{ \begin{aligned} \varepsilon_\alpha^1 \\ \gamma_{xy}^1 \end{aligned} \right\} + f(z) \left\{ \begin{aligned} \varepsilon_\alpha^2 \\ \gamma_{xy}^2 \end{aligned} \right\}, \tag{4}$$

$$\gamma_{\alpha z} = g(z)\gamma_{\alpha z}^0, \quad \varepsilon_z = g'(z)\varepsilon_z^0,$$

where

$$\varepsilon_\alpha^0 = \frac{\partial u_\alpha}{\partial \alpha}, \quad \varepsilon_\alpha^1 = -\frac{\partial^2 u_z}{\partial \alpha^2}, \quad \varepsilon_\alpha^2 = \frac{\partial \phi_\alpha}{\partial \alpha}, \quad \gamma_{\alpha z}^0 = \frac{\partial \phi_z}{\partial \alpha} + \phi_\alpha, \quad \varepsilon_z^0 = \phi_z, \tag{5}$$

$$\gamma_{xy}^0 = \frac{\partial u_y}{\partial x} + \frac{\partial u_x}{\partial y}, \quad \gamma_{xy}^1 = -2\frac{\partial^2 u_z}{\partial x \partial y}, \quad \gamma_{xy}^2 = \frac{\partial \phi_y}{\partial x} + \frac{\partial \phi_x}{\partial y}.$$

In addition, the load-displacement formula between the plate and the supporting foundations is expressed according to the three-parameter Visco-Winkler-Pasternak model by

$$R = \left(k_w - k_s \nabla^2 + c_d \frac{\partial}{\partial t} \right) u_z, \tag{6}$$

where R is the foundation reaction per unit area, k_w and k_s are Winkler’s and Pasternak’s foundation stiffnesses, respectively, and ∇^2 represents Laplace’s operator. In addition, c_d refers to the damping coefficient. Some special models may be simply obtained from the present models as:

- Winkler’s model: $k_s = 0, c_d = 0$.
- Pasternak’s model: $k_w = 0, c_d = 0$.
- Winkler-Pasternak’s model: $c_d = 0$.
- Visco-Winkler’s model: $k_s = 0$.
- Visco-Pasternak’s model: $k_w = 0$.

2.3. Constitutive Equations

For transverse shear and normal strain in the FG plate coordinates, the stress-strain relationships can be expressed as

$$\begin{pmatrix} \sigma_x \\ \sigma_y \\ \sigma_z \\ \tau_{yz} \\ \tau_{xz} \\ \tau_{xy} \end{pmatrix} = \begin{bmatrix} c_{11} & c_{12} & c_{13} & 0 & 0 & 0 \\ & c_{22} & c_{23} & 0 & 0 & 0 \\ & & c_{33} & 0 & 0 & 0 \\ & & & c_{44} & 0 & 0 \\ & \text{symm.} & & & c_{55} & 0 \\ & & & & & c_{66} \end{bmatrix} \begin{pmatrix} \varepsilon_x \\ \varepsilon_y \\ \varepsilon_z \\ \gamma_{yz} \\ \gamma_{xz} \\ \gamma_{xy} \end{pmatrix}, \tag{7}$$

where $c_{ij}(z)$ are given by

$$\begin{aligned} c_{11}(z) = c_{22}(z) = c_{33}(z) &= \frac{(1-\nu)E(z)}{(1-2\nu)(1+\nu)}, \\ c_{12}(z) = c_{13}(z) = c_{23}(z) &= \frac{\nu E(z)}{(1-2\nu)(1+\nu)}, \\ c_{44}(z) = c_{55}(z) = c_{66}(z) &= \frac{E(z)}{2(1+\nu)}, \end{aligned} \tag{8}$$

in which $E(z)$ is Young’s modulus and ν is Poisson’s ratio.

2.4. Stress Resultants

For transverse shear and normal strain in the FG plate coordinates, the stress-strain relationships can be expressed as

$$\begin{aligned} \{ (N_x, M_x, S_x), (N_{xy}, M_{xy}, S_{xy}) \} &= \int_{-h/2}^{h/2} (1, z, f(z)) \{ \sigma_x, \tau_{xy} \} dz, \\ S_z &= \int_{-h/2}^{h/2} g'(z) \sigma_z dz, \\ \{ Q_x, Q_y \} &= \int_{-h/2}^{h/2} g(z) \{ \tau_{xz}, \tau_{yz} \} dz. \end{aligned} \tag{9}$$

Using expressions (3)–(7) in Equation (8), expressions for stress resultants (N_x, N_y, N_{xy}), moments (M_x, M_y, M_{xy}), shape moments (S_x, S_y, S_{xy}), and shear forces (Q_x, Q_y) can be obtained. These expressions are given by:

$$\begin{pmatrix} \mathcal{N} \\ \mathcal{M} \\ \mathcal{S} \\ S_z \end{pmatrix} = \begin{bmatrix} \mathcal{B} & \overline{\mathcal{B}} & \overline{\overline{\mathcal{B}}} & \mathcal{H} \\ & \mathcal{D} & \overline{\mathcal{D}} & \overline{\mathcal{H}} \\ & & \overline{\mathcal{D}} & \overline{\mathcal{H}} \\ \text{symm.} & & & A_{33} \end{bmatrix} \begin{pmatrix} \varepsilon^0 \\ \varepsilon^1 \\ \varepsilon^2 \\ \varepsilon_z^0 \end{pmatrix}, \quad \begin{pmatrix} Q_y \\ Q_x \end{pmatrix} = \begin{bmatrix} A_{44} & 0 \\ 0 & A_{55} \end{bmatrix} \begin{pmatrix} \gamma_{yz}^0 \\ \gamma_{xz}^0 \end{pmatrix}, \tag{10}$$

where

$$\mathcal{N} = \begin{Bmatrix} N_x \\ N_y \\ N_{xy} \end{Bmatrix}, \mathcal{M} = \begin{Bmatrix} M_x \\ M_y \\ M_{xy} \end{Bmatrix}, \mathcal{S} = \begin{Bmatrix} N_x \\ N_y \\ S_{xy} \end{Bmatrix}, \varepsilon^0 = \begin{Bmatrix} \varepsilon_x^0 \\ \varepsilon_y^0 \\ \gamma_{xy}^0 \end{Bmatrix}, \varepsilon^1 = \begin{Bmatrix} \varepsilon_x^1 \\ \varepsilon_y^1 \\ \gamma_{xy}^1 \end{Bmatrix}, \varepsilon^2 = \begin{Bmatrix} \varepsilon_x^2 \\ \varepsilon_y^2 \\ \gamma_{xy}^2 \end{Bmatrix}, \quad (11)$$

$$\mathcal{B} = \begin{bmatrix} B_{11} & B_{12} & 0 \\ B_{12} & B_{22} & 0 \\ 0 & 0 & B_{66} \end{bmatrix}, \bar{\mathcal{B}} = \begin{bmatrix} \bar{B}_{11} & \bar{B}_{12} & 0 \\ \bar{B}_{12} & \bar{B}_{22} & 0 \\ 0 & 0 & \bar{B}_{66} \end{bmatrix}, \bar{\bar{\mathcal{B}}} = \begin{bmatrix} \bar{\bar{B}}_{11} & \bar{\bar{B}}_{12} & 0 \\ \bar{\bar{B}}_{12} & \bar{\bar{B}}_{22} & 0 \\ 0 & 0 & \bar{\bar{B}}_{66} \end{bmatrix}, \quad (12)$$

$$\mathcal{D} = \begin{bmatrix} D_{11} & D_{12} & 0 \\ D_{12} & D_{22} & 0 \\ 0 & 0 & D_{66} \end{bmatrix}, \bar{\mathcal{D}} = \begin{bmatrix} \bar{D}_{11} & \bar{D}_{12} & 0 \\ \bar{D}_{12} & \bar{D}_{22} & 0 \\ 0 & 0 & \bar{D}_{66} \end{bmatrix}, \bar{\bar{\mathcal{D}}} = \begin{bmatrix} \bar{\bar{D}}_{11} & \bar{\bar{D}}_{12} & 0 \\ \bar{\bar{D}}_{12} & \bar{\bar{D}}_{22} & 0 \\ 0 & 0 & \bar{\bar{D}}_{66} \end{bmatrix}, \quad (13)$$

$$\mathcal{H} = \begin{bmatrix} H_{13} \\ H_{23} \\ 0 \end{bmatrix}, \bar{\mathcal{H}} = \begin{bmatrix} \bar{H}_{13} \\ \bar{H}_{23} \\ 0 \end{bmatrix}, \bar{\bar{\mathcal{H}}} = \begin{bmatrix} \bar{\bar{H}}_{13} \\ \bar{\bar{H}}_{23} \\ 0 \end{bmatrix}, \quad (14)$$

in which $B_{ij}, \bar{B}_{ij}, \dots$ etc., are the plate stiffness, defined by

$$\left. \begin{aligned} \left\{ B_{ij}, \bar{B}_{ij}, \bar{\bar{B}}_{ij} \right\} &= \int_{-h/2}^{h/2} c_{ij}(z) \{1, z, f(z)\} dz \\ \left\{ D_{ij}, \bar{D}_{ij}, \bar{\bar{D}}_{ij} \right\} &= \int_{-h/2}^{h/2} c_{ij}(z) \{z^2, zf(z), [f(z)]^2\} dz \\ \left\{ H_{\alpha 3}, \bar{H}_{\alpha 3}, \bar{\bar{H}}_{\alpha 3} \right\} &= \int_{-h/2}^{h/2} c_{\alpha 3}(z) g'(z) \{1, z, f(z)\} dz, \alpha = 1, 2, \\ \left\{ A_{33}, A_{rr} \right\} &= \int_{-h/2}^{h/2} \{c_{33}(z)[g'(z)]^2, c_{rr}(z)[g(z)]^2\} dz, r = 4, 5. \end{aligned} \right\} i, j = 1, 2, 6, \quad (15)$$

Hamilton’s principle can be written as

$$\delta \int_{t_1}^{t_2} (T - U) dt = 0, \quad (16)$$

where the first variation of the kinetic energy T is represented as

$$\delta T = - \iint_{\Omega} \int_{-h/2}^{h/2} \rho \ddot{v}_i \delta v_i dz d\Omega, \quad (17)$$

and U is the total potential energy represented as

$$\delta U = \iint_{\Omega} \left[\int_{-h/2}^{h/2} (\sigma_i \delta \varepsilon_i + \tau_{ij} \delta \gamma_{ij}) dz + R \delta v_z \right] d\Omega. \quad (18)$$

Using Equations (2), (4), (7), (17), and (18) in Equation (16) and carrying out the first variation allows us to get the following governing equations associated with the present quasi-3D plate theory:

$$\delta u_x : N_{x,x} + N_{xy,y} = I_0 \ddot{u}_x - I_1 \ddot{u}_{z,x} + I_3 \ddot{\phi}_x, \quad (19)$$

$$\delta u_y : N_{xy,x} + N_{y,y} = I_0 \ddot{u}_y - I_1 \ddot{u}_{z,y} + I_3 \ddot{\phi}_y, \quad (20)$$

$$\delta u_z : M_{x,xx} + 2M_{xy,xy} + M_{y,yy} - R = I_0 \ddot{u}_z + I_1 (\ddot{u}_{x,x} + \ddot{u}_{y,y}) - I_2 \nabla^2 \ddot{u}_z + I_4 (\ddot{\phi}_{x,x} + \ddot{\phi}_{y,y}) + I_6 \ddot{\phi}_z, \quad (21)$$

$$\delta \phi_x : S_{x,x} + S_{xy,y} - Q_x = I_3 \ddot{u}_x - I_4 \ddot{u}_{z,x} + I_5 \ddot{\phi}_x, \quad (22)$$

$$\delta\phi_y : S_{xy,x} + S_{y,y} - Q_y = I_3\ddot{u}_y - I_4\ddot{u}_{z,y} + I_5\ddot{\phi}_y, \tag{23}$$

$$u_z : Q_{x,x} + Q_{y,y} - S_z = I_6\ddot{u}_z + I_7\ddot{\phi}_z, \tag{24}$$

where

$$\{I_0, I_1, I_2, I_3, I_4, I_5, I_6, I_7\} = \int_{-h/2}^{h/2} \rho(z) \{1, z, z^2, f, zf, f^2, g, g^2\} dz. \tag{25}$$

The following closed-form solution is appropriate for such simply-supported plates and is seen to satisfy all governing equations:

$$\begin{pmatrix} (u_x, \phi_x) \\ (u_y, \phi_y) \\ (u_z, \phi_z) \end{pmatrix} = \sum_{l=1}^{\infty} \sum_{m=1}^{\infty} \begin{pmatrix} (U_{ij}, X_{ij}) \cos(\lambda x) \sin(\mu y) \\ (V_{ij}, Y_{ij}) \sin(\lambda x) \cos(\mu y) \\ (W_{ij}, Z_{ij}) \sin(\lambda x) \sin(\mu y) \end{pmatrix} e^{-i\omega t}, \tag{26}$$

where $\lambda = i\pi/a$ and $\mu = j\pi/b$. In addition, i and j represent the mode shapes of vibration and they indicate the number of half-waves in x - and y -directions, respectively. The stress and moment resultants in Equations (11)–(14) may be represented as

$$\begin{aligned} N_x &= B_{11} \frac{\partial u_x}{\partial x} + B_{12} \frac{\partial u_y}{\partial y} - \bar{B}_{11} \frac{\partial^2 w_b}{\partial x^2} - \bar{B}_{12} \frac{\partial^2 w_b}{\partial y^2} - \bar{B}_{11} \frac{\partial^2 w_s}{\partial x^2} - \bar{B}_{12} \frac{\partial^2 w_s}{\partial y^2} + H_{13} u_z, \\ N_y &= B_{12} \frac{\partial u_x}{\partial x} + B_{22} \frac{\partial u_y}{\partial y} - \bar{B}_{12} \frac{\partial^2 w_b}{\partial x^2} - \bar{B}_{22} \frac{\partial^2 w_b}{\partial y^2} - \bar{B}_{12} \frac{\partial^2 w_s}{\partial x^2} - \bar{B}_{22} \frac{\partial^2 w_s}{\partial y^2} + H_{23} u_z, \\ N_{xy} &= B_{66} \left(\frac{\partial u_y}{\partial x} + \frac{\partial u_x}{\partial y} \right) - 2\bar{B}_{66} \frac{\partial^2 w_b}{\partial x \partial y} - 2\bar{B}_{66} \frac{\partial^2 w_s}{\partial x \partial y}, \\ M_x &= \bar{B}_{11} \frac{\partial u_x}{\partial x} + \bar{B}_{12} \frac{\partial u_y}{\partial y} - D_{11} \frac{\partial^2 w_b}{\partial x^2} - D_{12} \frac{\partial^2 w_b}{\partial y^2} - \bar{D}_{11} \frac{\partial^2 w_s}{\partial x^2} - \bar{D}_{12} \frac{\partial^2 w_s}{\partial y^2} + \bar{H}_{13} u_z, \\ M_y &= \bar{B}_{12} \frac{\partial u_x}{\partial x} + \bar{B}_{22} \frac{\partial u_y}{\partial y} - D_{12} \frac{\partial^2 w_b}{\partial x^2} - D_{22} \frac{\partial^2 w_b}{\partial y^2} - \bar{D}_{12} \frac{\partial^2 w_s}{\partial x^2} - \bar{D}_{22} \frac{\partial^2 w_s}{\partial y^2} + \bar{H}_{23} u_z, \\ M_{xy} &= \bar{B}_{66} \left(\frac{\partial u_y}{\partial x} + \frac{\partial u_x}{\partial y} \right) - 2D_{66} \frac{\partial^2 w_b}{\partial x \partial y} - 2\bar{D}_{66} \frac{\partial^2 w_s}{\partial x \partial y}, \\ S_x &= \bar{B}_{11} \frac{\partial u_x}{\partial x} + \bar{B}_{12} \frac{\partial u_y}{\partial y} - \bar{D}_{11} \frac{\partial^2 w_b}{\partial x^2} - \bar{D}_{12} \frac{\partial^2 w_b}{\partial y^2} - \bar{D}_{11} \frac{\partial^2 w_s}{\partial x^2} - \bar{D}_{12} \frac{\partial^2 w_s}{\partial y^2} + \bar{H}_{13} u_z, \\ S_y &= \bar{B}_{12} \frac{\partial u_x}{\partial x} + \bar{B}_{22} \frac{\partial u_y}{\partial y} - \bar{D}_{12} \frac{\partial^2 w_b}{\partial x^2} - \bar{D}_{22} \frac{\partial^2 w_b}{\partial y^2} - \bar{D}_{12} \frac{\partial^2 w_s}{\partial x^2} - \bar{D}_{22} \frac{\partial^2 w_s}{\partial y^2} + \bar{H}_{23} u_z, \\ S_{xy} &= \bar{B}_{66} \left(\frac{\partial u_y}{\partial x} + \frac{\partial u_x}{\partial y} \right) - 2\bar{D}_{66} \frac{\partial^2 w_b}{\partial x \partial y} - 2\bar{D}_{66} \frac{\partial^2 w_s}{\partial x \partial y}, \\ Q_x &= A_{55} \frac{\partial(w_s + u_z)}{\partial x}, \quad Q_y = A_{44} \frac{\partial(w_s + u_z)}{\partial y}. \end{aligned} \tag{27}$$

The governing Equations (19)–(24) after using Equations (26) and (27) are reduced to

$$([\mathcal{K}] - i\omega[\mathcal{R}] - \omega^2[\mathcal{P}]) \{\Delta\} = \{0\}, \tag{28}$$

where $\{\Delta\} = \{u_x, u_y, u_z, \phi_x, \phi_y, \phi_z\}^T$ and the non-zero elements K_{kl} of the symmetric matrix $[\mathcal{K}]$ and P_{kl} of the symmetric matrix $[\mathcal{P}]$ are defined for FG plates by

$$\begin{aligned}
 K_{11} &= B_{11}\lambda^2 + B_{66}\mu^2, K_{12} = (B_{12} + B_{66})\lambda\mu, K_{13} = -\lambda[\bar{B}_{11}\lambda^2 + (\bar{B}_{12} + 2\bar{B}_{66})\mu^2], \\
 K_{14} &= \bar{\bar{B}}_{11}\lambda^2 + \bar{\bar{B}}_{66}\mu^2, K_{15} = \left(\bar{\bar{B}}_{12} + \bar{\bar{B}}_{66}\right)\lambda\mu, K_{16} = -H_{13}\lambda, K_{22} = B_{66}\lambda^2 + B_{22}\mu^2, \\
 K_{23} &= -\mu[(\bar{B}_{12} + 2\bar{B}_{66})\lambda^2 + \bar{B}_{22}\mu^2], K_{24} = K_{15}, K_{25} = \bar{\bar{B}}_{66}\lambda^2 + \bar{\bar{B}}_{22}\mu^2, \\
 K_{26} &= -H_{23}\mu, K_{33} = D_{11}\lambda^4 + 2(D_{12} + 2D_{66})\lambda^2\mu^2 + D_{22}\mu^4 + k_s(\lambda^2 + \mu^2) + k_w, \\
 K_{34} &= -\lambda[\bar{D}_{11}\lambda^2 + (\bar{D}_{12} + 2\bar{D}_{66})\mu^2], K_{35} = -\mu[(\bar{D}_{12} + 2\bar{D}_{66})\lambda^2 + \bar{D}_{22}\mu^2], \\
 K_{36} &= \bar{H}_{13}\lambda^2 + \bar{H}_{23}\mu^2, K_{44} = \bar{\bar{D}}_{11}\lambda^2 + \bar{\bar{D}}_{66}\mu^2 + A_{55}, K_{45} = \left(\bar{\bar{D}}_{12} + \bar{\bar{D}}_{66}\right)\lambda\mu, \\
 K_{46} &= \left(A_{55} - \bar{\bar{H}}_{13}\right)\lambda, K_{55} = \bar{\bar{D}}_{66}\lambda^2 + \bar{\bar{D}}_{22}\mu^2 + A_{44}, K_{56} = \left(A_{44} - \bar{\bar{H}}_{23}\right)\mu, \\
 K_{66} &= A_{55}\lambda^2 + A_{44}\mu^2 + A_{33}, P_{11} = P_{22} = I_0, P_{13} = -I_1\lambda, P_{14} = P_{25} = I_3, \\
 P_{23} &= -I_1\mu, P_{33} = I_0 + I_2(\lambda^2 + \mu^2), P_{34} = -I_4\lambda, P_{35} = -I_4\mu, P_{36} = I_6, \\
 P_{44} &= P_{55} = I_5, P_{66} = I_7, R_{33} = c_d.
 \end{aligned} \tag{29}$$

3. Numerical Results and Discussion

This section presents some numerical examples for vibration frequencies of isotropic and FG rectangular plates. The accuracy and efficiency of the present quasi-3D refined theory in predicting fundamental and natural frequencies of simply-supported plates are discussed. The results due to the present theory are compared with those found in the literature using various theories. Different material properties are assumed as follows:

3.1. Isotropic Plate

$$\nu = 0.3. \tag{30}$$

3.2. Functionally Graded Plates

$$\text{Aluminum (Al)} : E_m = 70 \text{ GPa}, \nu = 0.3, \rho_m = 2703 \text{ kg/m}^3, \tag{31}$$

$$\text{Alumina (Al}_2\text{O}_3) : E_c = 380 \text{ GPa}, \nu = 0.3, \rho_c = 3800 \text{ kg/m}^3, \tag{32}$$

$$\text{Zirconia (ZrO}_2) : E_c = 200 \text{ GPa}, \nu = 0.3, \rho_c = 5700 \text{ kg/m}^3. \tag{33}$$

Numerical results concern values of dimensionless fundamental and natural frequencies are displayed in Tables 1–18. Different forms for dimensionless frequencies and foundation parameters are considered.

3.3. Analysis of Isotropic Plates

In this section, the special case of homogeneous isotropic plates is analyzed. Tables 1–4 present the results of the non-dimensional natural frequency obtained by the present quasi-3D theory for square plates. In Tables 1–4, the non-dimensional natural frequencies and nondimensional coefficients of foundations are utilized as

$$\bar{\omega} = \omega a^2 \sqrt{\frac{\rho_0 h}{D_0}}, D_0 = \frac{E_0 h^3}{12(1 - \nu^2)}, \tag{34}$$

in which E_0, ν, ρ_0 denote Young’s modulus, Poisson’s ratio, and density of the isotropic material.

Table 1 presents the natural frequencies of isotropic square plates due to the first eight modes. These frequencies are compared with the solutions of different authors: the 3D exact solutions by Leissa [29], Zhou et al. [30], Nagino et al. [31]; the FSDT using differential quadrature element method (DQM) by Liu and Liew [32]; and HDTs by Hosseini-Hashemi et al. [33], Shufrin et al. [34], Akavci [35], and a quasi-3D hybrid type HSDT by Mantari et al. [36].

Table 1. Non-dimensional natural frequencies $\bar{\omega} = \omega a^2 \sqrt{\rho h / D_0}$ for isotropic square plates.

<i>a/h</i>	Theory	Mode							
		(1,1)	(1,2)	(2,1)	(2,2)	(1,3)	(3,1)	(2,3)	(3,2)
1000	Leissa [29]	19.7392	49.3480	49.3480	78.9568	98.6960	98.6960	128.3021	128.3021
	Zhou et al. [30]	19.7115	49.3470	49.3470	78.9528	98.6911	98.6911	128.3048	128.3048
	Akavci [35]	19.7391	49.3476	49.3476	78.9557	98.6943	98.6943	128.3020	128.3020
	Mantari et al. [36]	19.7396	49.3482	49.3482	78.9568	98.6956	98.6956	128.3036	128.3036
	Present	19.73914	49.34760	49.34760	78.95574	98.69434	98.69434	128.30197	128.30197
100	Leissa [29]	19.7319	49.3027	49.3027	78.8410	98.5150	98.5150	127.9993	127.9993
	Nagino et al. [31]	19.7320	49.3050	49.3050	78.8460	98.5250	98.5250	128.0100	128.0100
	Akavci [35]	19.7322	49.3045	49.3045	78.8456	98.5223	98.5223	128.0120	128.0120
	Mantari et al. [36]	19.7326	49.3055	49.3055	78.8475	98.5250	98.5250	128.0156	128.0156
	Present	19.73231	49.30491	49.30491	78.84657	98.52386	98.52386	128.01415	128.01415
10	Liu et al. [32]	19.0584	45.4478	45.4478	69.7167	84.9264	84.9264	106.5154	106.5154
	Hosseini et al. [33]	19.0653	45.4869	45.4869	69.8093	85.0646	85.0646	106.7350	106.7350
	Akavci [35]	19.0850	45.5957	45.5957	70.0595	85.4315	85.4315	107.3040	107.3040
	Mantari et al. [36]	19.0901	45.6200	45.6200	70.1083	85.4964	85.4964	107.3896	107.3896
	Present	19.09028	45.62185	45.62185	70.11284	85.50305	85.50305	107.39973	107.39973
5	Shufrin et al. [34]	17.4524	38.1884	38.1884	55.2539	65.3130	65.3130	78.9864	78.9864
	Hosseini et al. [33]	17.4523	38.1883	38.1883	55.2543	65.3135	65.3135	78.9865	78.9865
	Akavci [35]	17.5149	38.4722	38.4722	55.8358	66.1207	66.1207	80.1637	80.1637
	Mantari et al. [36]	17.5271	38.4991	38.4991	55.8410	66.0874	66.0874	80.0364	80.0364
	Present	17.52821	38.50383	38.50383	55.84950	66.09809	66.09809	80.04976	80.04976

It is clear from Table 1 that for the value of the side-to-thickness ratio ($a/h = 1000$), the first mode of the present frequency is identical to those given by Leissa [29] and Akavci [35] and has proximity with the one obtained by Mantari et al. [36]. Additionally, the high modes of the present natural frequencies are identical to those given by Akavci [35] and are very close to the ones obtained by Zhou et al. [30], Leissa [29], and Mantari et al. [36]. For the side-to-thickness ratio ($a/h = 100$), it is noted that the results are slightly less than those predicted by Mantari et al. [36] and slightly greater than those predicted by Leissa [29], Nagino et al. [31], and Akavci [35]. For moderately thick plates ($a/h = 10$), the present natural frequencies are very close to those obtained by Mantari et al. [36] and slightly greater than those predicted by Liu et al. [32], Hosseini et al. [33], and Akavci [35]. For thin plates ($a/h = 5$), the present natural frequencies are close to those obtained by Akavci [35] and Mantari et al. [36].

In Tables 2–4, the outcomes of the non-dimensional natural frequency $\bar{\omega}$ represented in Equation (34) for isotropic square plates resting on visco–Pasternak foundations are reported. The nondimensional coefficients of the three-parameter foundations are utilized as

$$\bar{k}_w = \frac{a^4}{D_0} k_w, \bar{k}_s = \frac{a^2}{D_0} k_s, \bar{c}_d = c_d h \sqrt{\frac{h}{\rho_0 D_0}}. \tag{35}$$

The most important case is considered for isotropic square plates resting on the two-parameter Pasternak foundation. However, additional results for plates resting on three-parameter visco–Pasternak foundations are also included for future comparisons. Different values for the three-parameter coefficients \bar{k}_w , \bar{k}_s , and \bar{c}_d are discussed.

Table 2. Non-dimensional fundamental frequencies $\bar{\omega} = \omega a^2 \sqrt{\rho h / D_0}$ for isotropic square plates resting on Visco-Winkler-Pasternak foundations ($a/h = 5, i = j = 1$).

\bar{k}_w	\bar{k}_s	Matsunaga [37]	Thai and Choi [38]	Mantari et al. [36]	Present			
					$\bar{c}_d = 0$	$\bar{c}_d = 0.5$	$\bar{c}_d = 1$	$\bar{c}_d = 1.5$
0	0	17.5260	17.4523	17.5271	17.52821	—	—	—
10		17.7847	17.7248	17.7858	17.78691	17.80266	17.85029	17.93085
10 ²		19.9528	20.0076	19.9613	19.96234	19.98001	20.03340	20.12372
10 ³		34.3395	35.5039	34.7796	34.78009	34.81060	34.90277	35.05861
10 ⁴		45.5260	45.5255	45.5260	45.52600	45.52600	45.52600	45.52600
10 ⁵		45.5260	45.5255	45.5260	45.52600	45.52600	45.52600	45.52600
0	10	22.0429	22.2145	22.0707	22.07157	22.09109	22.15007	22.24983
10		22.2453	22.4286	22.2757	22.27657	22.29627	22.35578	22.45646
10 ²		23.9830	24.2723	24.0401	24.04090	24.06214	24.12631	24.23485
10 ³		36.6276	38.0650	37.2169	37.21732	37.24990	37.34833	37.51475
10 ⁴		45.5260	45.5255	45.5260	45.52600	45.52600	45.52600	45.52600
10 ⁵		45.5260	45.5255	45.5260	45.52600	45.52600	45.52600	45.52600

Table 3. Non-dimensional natural frequencies $\bar{\omega} = \omega a^2 \sqrt{\rho h / D_0}$ for isotropic square plates resting on Visco-Winkler-Pasternak foundations ($a/h = 5, i = 1, j = 2$).

\bar{k}_w	\bar{k}_s	Matsunaga [37]	Thai and Choi [38]	Mantari et al. [36]	Present			
					$\bar{c}_d = 0$	$\bar{c}_d = 1$	$\bar{c}_d = 2$	$\bar{c}_d = 3$
0	0	38.4827	38.1883	38.4991	38.50383	—	—	—
10		38.5929	38.3098	38.6093	38.61403	38.75920	39.21005	40.01800
10 ²		39.5669	39.3895	39.5860	39.59068	39.73930	40.20086	41.02792
10 ³		47.8667	48.8772	48.1688	48.17300	48.35118	48.90436	49.89463
10 ⁴		71.9829	71.9829	71.9829	71.98293	71.98293	71.98293	71.98293
10 ⁵		71.9829	71.9829	71.9829	71.98293	71.98293	71.98293	71.98293
0	10	43.4816	43.7943	43.5741	43.57850	43.74104	44.24576	45.14976
10		43.5747	43.9009	43.6701	43.67455	43.83742	44.34317	45.24900
10 ²		44.3994	44.8445	44.5241	44.52853	44.69434	45.20920	46.13126
10 ³		51.6029	53.3580	52.2029	52.20676	52.39828	52.99275	54.05639
10 ⁴		71.9829	71.9829	71.9829	71.98293	71.98293	71.98293	71.98293
10 ⁵		71.9829	71.9829	71.9829	71.98293	71.98293	71.98293	71.98293

The first three non-dimensional natural frequencies of a thicker square plate ($a/h = 5$) resting on the elastic foundation are presented in Tables 2–4. The first mode ($i = j = 1$) fundamental frequencies $\bar{\omega}_{11}$ are represented in Table 2 while natural frequencies $\bar{\omega}_{12}$ and $\bar{\omega}_{13}$ are presented in Tables 3 and 4, respectively. In such tables, the frequencies are compared with the refined shear deformation theory given by Thai and Choi [38], the HSDT proposed by Matsunaga [37], and a quasi-3D hybrid type HSDT by Mantari et al. [36]

Table 4. Non-dimensional natural frequencies $\bar{\omega} = \omega a^2 \sqrt{\rho h / D_0}$ for isotropic square plates resting on Visco-Winkler-Pasternak foundations ($a/h = 5, i = 1, j = 3$).

\bar{k}_w	\bar{k}_s	Matsunaga [37]	Thai and Choi [38]	Mantari et al. [36]	Present			
					$\bar{c}_d = 0$	$\bar{c}_d = 1$	$\bar{c}_d = 2$	$\bar{c}_d = 3$
0	0	65.9961	65.3135	66.0874	66.09809	—	—	—
10		66.0569	65.3841	66.1481	66.15875	66.40586	67.17631	68.56834
10 ²		66.5995	66.0138	66.6907	66.70143	66.95005	67.72517	69.12547
10 ³		71.5577	72.0036	71.8192	71.83050	72.09271	72.90970	74.38380
10 ⁴		97.4964	101.7990	101.7992	101.79924	101.79924	101.79924	101.79924
10 ⁵		101.7992	101.7990	101.7992	101.79924	101.79924	101.79924	101.79924
0	10	71.4914	71.9198	71.7485	71.75974	72.02177	72.83822	74.31135
10		71.5423	71.9839	71.8028	71.81402	72.07618	72.89304	74.36692
10 ²		71.9964	72.5554	72.2886	72.29990	72.56328	73.38389	74.86433
10 ³		76.1848	78.0290	76.9124	76.92383	77.19813	78.05223	79.59112
10 ⁴		99.0187	101.7990	101.7992	101.79924	101.79924	101.79924	101.79924
10 ⁵		101.7992	101.7990	101.7992	101.79924	101.79924	101.79924	101.79924

The fundamental frequencies in Table 2 are close to those obtained by Matsunaga [37] and Mantari et al. [36] and slightly greater than those of Thai and Choi [38]. It is clear that the frequencies increase as the two-parameter coefficients increase. For higher values of the first parameter coefficient \bar{k}_w , the frequencies still have the same values. The inclusion of the third-parameter coefficient \bar{c}_d is also discussed here. It is interesting to see that the frequencies increase with the increase in the value of \bar{c}_d .

The natural frequencies in Tables 3 and 4 are also closer to those obtained by Matsunaga [37] and Mantari et al. [36] and slightly greater than those of Thai and Choi [38]. Once again, the frequencies increase as the three-parameter coefficients increase. For higher values of the first parameter coefficient \bar{k}_w the frequencies still have the same values. It is to be noted that in Tables 2–4, as the mode m increases, the frequency increases irrespective of the values of the three-parameter coefficients.

3.4. Analysis of FG Plates

Here, the non-dimensional fundamental frequencies of FG square plates are discussed in Tables 5 and 6. The FG plates are fabricated of different materials. The mechanical properties of such materials are given in Equations (31)–(33). The non-dimensional frequency is utilized as

$$\hat{\omega} = \omega h \sqrt{\frac{\rho_m}{E_m}} \tag{36}$$

The non-dimensional fundamental frequencies $\hat{\omega}_{11}$ for thicker ($a/h = 5$) Aluminum-Zirconia (Al/ZrO₂) FG square plates without elastic foundations are compared with the corresponding results in Table 5. Additional results for plates resting on Visco-Winkler-Pasternak foundations are also presented. The nondimensional coefficients of the three-parameter foundations are utilized as

$$\bar{k}_w = \frac{a^4}{D_m} k_w, \bar{k}_s = \frac{a^2}{D_m} k_s, \bar{c}_d = c_d h \sqrt{\frac{h}{\rho_m D_m}}, D_m = \frac{E_m h^3}{12(1 - \nu^2)} \tag{37}$$

In Table 5, the fundamental frequencies for three values of the FG power-law index p are computed and compared with the 3D exact solution by Vel et al. [39], quasi-3D sinusoidal and hyperbolic HSDTs by Neves et al. [40,41], a quasi-3D hybrid type HSDT by Mantari et al. [36], and HSDTs by Akavci [35], Hosseini-Hashemi et al. [32], and Matsunaga [42]. The frequencies increase with the increase in the FG power-law index p . Neglecting the three-parameter foundation coefficients shows that the present frequencies are identical to those of Mantari et al. [36]. In addition, the present frequencies agree well with the HSDTs’ frequencies. For the sake of future comparison, some frequencies for plates

on the Visco-Winkler-Pasternak foundation are also included in the same table. Once again, the frequencies increase with the increase in the three-parameter foundation coefficients.

Table 5. Non-dimensional fundamental frequencies $\hat{\omega} = \omega h \sqrt{\rho_m/E_m}$ for Al/ZrO₂ FG square plates resting on Visco-Winkler-Pasternak foundations ($a/h = 5$).

Theory	p			
	2	3	5	
Vel and Batra [39]	0.2197	0.2211	0.2225	
Neves et al. ($\epsilon_z = 0$) [40]	0.2189	0.2202	0.2215	
Neves et al. ($\epsilon_z \neq 0$) [40]	0.2198	0.2212	0.2225	
Neves et al. ($\epsilon_z = 0$) [41]	0.2191	0.2205	0.2220	
Neves et al. ($\epsilon_z \neq 0$) [41]	0.2201	0.2216	0.2230	
Hosseini-Hashemi et al. [33]	0.2264	0.2276	0.2291	
Akavci [35]	0.2263	0.2268	0.2277	
Matsunaga [42]	0.2264	0.2270	0.2280	
Mantari et al. [36]	0.2285	0.2290	0.2295	
Present	$\bar{k}_w = \bar{k}_s = \bar{c}_d = 0$	0.22848	0.22901	0.22952
	$\bar{k}_w = 10, \bar{k}_s = 0, \bar{c}_d = 0$	0.23062	0.23130	0.23199
	$\bar{k}_w = 10, \bar{k}_s = 10, \bar{c}_d = 0$	0.26937	0.27256	0.27610
	$\bar{k}_w = 10, \bar{k}_s = 10, \bar{c}_d = 1$	0.26976	0.27301	0.27664
	$\bar{k}_w = 10, \bar{k}_s = 10, \bar{c}_d = 2$	0.27095	0.27438	0.27825
	$\bar{k}_w = 10^2, \bar{k}_s = 10, \bar{c}_d = 2$	0.28694	0.29132	0.29627

The non-dimensional fundamental frequencies $\hat{\omega}_{11} = \omega h \sqrt{\rho_m/E_m}$ for Aluminum-Alumina (Al/Al₂O₃) FG rectangular plates are presented in Table 6. The frequencies are computed for four different values of the FG power-law index p and compared with a quasi-3D hybrid type HSDT by Mantari et al. [36] and a 3D exact solution proposed by Jin et al. [43]. Generally, the frequencies decrease with the increase in the FG power-law index p . Additionally, the frequencies increase as both a/h and b/a decrease. Neglecting the three-parameter foundation coefficients shows that the present frequencies give good accuracy with those in [36] and [43] for square plates ($b/a = 1$). However, for rectangular plates ($b/a = 2$), the present frequencies are very close to those of Mantari et al. [36] and slightly greater than those of Jin et al. [43]. For the sake of future comparison, some frequencies for plates on the Visco-Winkler-Pasternak foundation are also included in Table 6. The non-dimensional coefficients of the three-parameter foundations are given in Equation (37). For all cases studied, the frequencies increase with the increase in the three-parameter foundation coefficients.

Table 6. Non-dimensional fundamental frequencies $\hat{\omega} = \omega h \sqrt{\rho_m/E_m}$ for Al/Al₂O₃ FG rectangular plates on Visco-Winkler-Pasternak foundations.

b/a	a/h	Theory	p				
			0	1	2	5	
1	10	Jin et al. [43]	0.1135	0.0870	0.0789	0.0741	
		Mantari et al. [36]	0.1135	0.0882	0.0806	0.0755	
		Present	$\bar{k}_w = \bar{k}_s = \bar{c}_d = 0$	0.11350	0.08818	0.08057	0.07553
			$\bar{k}_w = 100, \bar{k}_s = 0, \bar{c}_d = 0.5$	0.11627	0.09230	0.08533	0.08090
			$\bar{k}_w = 0, \bar{k}_s = 10, \bar{c}_d = 0.5$	0.11889	0.09613	0.08969	0.08578
	$\bar{k}_w = 100, \bar{k}_s = 10, \bar{c}_d = 0.5$	0.12152	0.09991	0.09397	0.09051		

Table 6. Cont.

<i>b/a</i>	<i>a/h</i>	Theory	<i>p</i>				
			0	1	2	5	
1	5	Jin et al. [43]	0.4169	0.3222	0.2905	0.2676	
		Mantari et al. [36]	0.4168	0.3260	0.2961	0.2722	
		Present	$\bar{k}_w = \bar{k}_s = \bar{c}_d = 0$	0.41685	0.32605	0.29613	0.27221
			$\bar{k}_w = 100, \bar{k}_s = 0, \bar{c}_d = 0.5$	0.42816	0.34278	0.31556	0.29463
			$\bar{k}_w = 0, \bar{k}_s = 10, \bar{c}_d = 0.5$	0.43885	0.35824	0.33329	0.31481
	$\bar{k}_w = 100, \bar{k}_s = 10, \bar{c}_d = 0.5$	0.44956	0.37344	0.35056	0.33425		
	2	Jin et al. [43]	1.8470	1.4687	1.3095	1.1450	
		Mantari et al. [36]	1.8505	1.4774	1.3219	1.1551	
		Present	$\bar{k}_w = \bar{k}_s = \bar{c}_d = 0$	1.85081	1.47762	1.32213	1.15544
			$\bar{k}_w = 100, \bar{k}_s = 0, \bar{c}_d = 0.5$	1.93506	1.59673	1.46375	1.33166
			$\bar{k}_w = 0, \bar{k}_s = 10, \bar{c}_d = 0.5$	2.01192	1.70066	1.58405	1.47548
	$\bar{k}_w = 100, \bar{k}_s = 10, \bar{c}_d = 0.5$	2.08633	1.79759	1.69386	1.60293		
2	10	Jin et al. [43]	0.0719	0.0550	0.0499	0.0471	
		Mantari et al. [36]	0.0718	0.0557	0.0510	0.0479	
		Present	$\bar{k}_w = \bar{k}_s = \bar{c}_d = 0$	0.07181	0.05573	0.05097	0.04794
			$\bar{k}_w = 100, \bar{k}_s = 0, \bar{c}_d = 0.5$	0.07614	0.06209	0.05824	0.05605
			$\bar{k}_w = 0, \bar{k}_s = 10, \bar{c}_d = 0.5$	0.07711	0.06348	0.05981	0.05778
	$\bar{k}_w = 100, \bar{k}_s = 10, \bar{c}_d = 0.5$	0.08115	0.06912	0.06611	0.06466		
	5	Jin et al. [43]	0.2713	0.2088	0.1888	0.1754	
		Mantari et al. [36]	0.2712	0.2115	0.1926	0.1786	
		Present	$\bar{k}_w = \bar{k}_s = \bar{c}_d = 0$	0.27124	0.21151	0.19262	0.17861
			$\bar{k}_w = 100, \bar{k}_s = 0, \bar{c}_d = 0.5$	0.28875	0.23709	0.22197	0.21183
			$\bar{k}_w = 0, \bar{k}_s = 10, \bar{c}_d = 0.5$	0.29268	0.24266	0.22828	0.21885
	$\bar{k}_w = 100, \bar{k}_s = 10, \bar{c}_d = 0.5$	0.30894	0.26520	0.25347	0.24662		
2	Jin et al. [43]	0.9570	0.7937	0.7149	0.6168		
	Mantari et al. [36]	1.3040	1.0346	0.9293	0.8236		
	Present	$\bar{k}_w = \bar{k}_s = \bar{c}_d = 0$	1.30422	1.03469	0.92945	0.82385	
		$\bar{k}_w = 100, \bar{k}_s = 0, \bar{c}_d = 0.5$	1.42513	1.20475	1.12760	1.06040	
		$\bar{k}_w = 0, \bar{k}_s = 10, \bar{c}_d = 0.5$	1.45155	1.24029	1.16792	1.10679	
$\bar{k}_w = 100, \bar{k}_s = 10, \bar{c}_d = 0.5$	1.55824	1.37906	1.32259	1.28071			

The non-dimensional fundamental frequencies $\check{\omega}_{11} = (\omega a^2/h) \sqrt{\rho_m/E_m}$ for Aluminum-Zirconia (Al/ZrO₂) FG square plates resting on Visco-Winkler-Pasternak foundations are reported in Table 7. When $p = 0$, the frequency parameter tends to $\check{\omega}_{11} = (\omega a^2/h) \sqrt{\rho_c/E_c}$. The frequencies, without the three-parameter foundation coefficients, are compared with the 3D exact solutions proposed by Vel and Batra [39], HSDTs proposed by Akavci [35], a quasi-3D hybrid type HSDT by Mantari et al. [36], and Matsunaga [42]. In general, the frequencies increase as both p and a/h increase. The present frequencies are compared well with those reported in [36]. Additionally, the frequencies approach to the corresponding solutions obtained in [35,39,42]. If the Visco-Winkler-Pasternak foundations are taken into account, the frequencies increase. Once again, the non-dimensional coefficients of the three-parameter foundations are given in Equation (37).

Table 7. Non-dimensional fundamental frequencies $\tilde{\omega} = (\omega a^2/h) \sqrt{\rho_m/E_m}$ for Al/ZrO₂ FG square plates on Visco-Winkler-Pasternak foundations.

<i>p</i>	<i>a/h</i>	Vel and Batra [39]	Akavci [35]	Matsunaga [42]	Mantari et al. [36]	Present ($\bar{k}_w, \bar{k}_s, \bar{c}_d$)			
						(0,0,0)	(10,0,0.1)	(0,10,0.1)	(10,10,0.1)
0*	$\sqrt{10}$	4.6582	4.6569	4.6582	4.6601	4.66072	4.68987	5.20264	5.22844
	10	5.7769	5.7754	5.7769	5.7769	5.77698	5.80392	6.28692	6.31166
1	5	5.4806	5.7110	5.7123	5.7501	5.75043	5.79726	6.61170	6.65231
	10	5.9609	6.1924	6.1932	6.2365	6.23656	6.28244	7.08625	7.12659
	20	6.1076	6.3388	6.3390	6.3842	6.38419	6.42989	7.23208	7.27240
2	5	5.4923	5.6593	5.6599	5.7115	5.71197	5.76558	6.68866	6.73430
3	5	5.5285	5.6718	5.6757	5.7246	5.72519	5.78258	6.76582	6.81423
5	5	5.5632	5.6941	5.7020	5.7376	5.73811	5.79984	6.85123	6.90276

$$* \tilde{\omega} = (\omega a^2/h) \sqrt{\rho_c/E_c}$$

In Tables 8–10, the non-dimensional natural frequencies $\tilde{\omega}$ for Aluminum-Alumina (Al/Al₂O₃) FG rectangular plates (*b/a* = 2) resting on Visco-Winkler-Pasternak foundations are reported. Three values of the side-to-thickness ratio *a/h* = 5, 10, 20 are considered. The non-dimensional frequency and the non-dimensional coefficients of the three-parameter foundations are utilized as

$$\tilde{\omega} = \frac{\omega a^2}{h} \sqrt{\frac{\rho_c}{E_c}}, \bar{c}_d = c_d h \sqrt{\frac{h}{\rho_c D_c}}, \bar{k}_w = \frac{a^4}{D_c} k_w, \bar{k}_s = \frac{a^2}{D_c} k_s, D_c = \frac{E_c h^3}{12(1 - \nu^2)}. \quad (38)$$

Tables 8–10 present the first four non-dimensional natural frequencies $\tilde{\omega}_{11}, \tilde{\omega}_{12}, \tilde{\omega}_{13}$ and $\tilde{\omega}_{21}$ of FG plates for various values of the FG power-law index *p*. Firstly, the frequencies increase as both the mode number and side-to-thickness ratio *a/h* increase and as the FG power-law index *p* decreases. For $\bar{k}_w = \bar{k}_s = \bar{c}_d = 0$, the present frequencies are compared with the corresponding ones due to the HSDTs proposed by Akavci [35], Thai et al. [44], a quasi-3D hybrid type HSDT by Mantari et al. [36], and the FSDT utilized by Hosseini-Hashemi et al. [3]. The present frequencies are very close to those in [35,36] and slightly greater than those in [3,44]. Furthermore, it is shown that for different values of *a/h* the present frequencies get good agreements with the other theories. The frequencies, with the inclusion of the three-parameter foundation coefficients, are presented for future comparisons. The results represent benchmarks to help other investigators to assure their results for plates resting on three-parameter viscoelastic foundations. It is obvious that the frequency slightly increases when adding the three parameters of viscoelastic foundations one by one. The maximum frequencies occurred when all foundation coefficients are included.

Table 8. Non-dimensional natural frequencies $\tilde{\omega} = (\omega a^2/h)\sqrt{\rho_c/E_c}$ for Al/Al₂O₃ FG rectangular plates on Visco-Winkler-Pasternak foundations ($b/a = 2, a/h = 5$).

Mode	Theory	p						
		0	1	2	5	8	10	
(1,1)	Akavci [35]	3.4495	2.6529	2.3989	2.2275	2.1724	2.1455	
	Thai et al. [44]	3.4412	2.6475	2.3949	2.2272	2.1697	2.1407	
	Hosseini et al. [3]	3.4409	2.6473	2.4017	2.2528	2.1985	2.1677	
	Mantari et al. [36]	3.4513	2.6913	2.4508	2.2725	2.2032	2.1689	
	Present	$\bar{k}_w = \bar{k}_s = \bar{c}_d = 0$	3.45145	2.69138	2.45102	2.27273	2.20328	2.16887
		$\bar{k}_w = 10, \bar{k}_s = 0, \bar{c}_d = 0.1$	3.57401	2.87249	2.66011	2.51080	2.45332	2.42438
		$\bar{k}_w = 0, \bar{k}_s = 10, \bar{c}_d = 0.1$	4.74470	4.43132	4.37556	4.37628	4.37573	4.37110
$\bar{k}_w = 10, \bar{k}_s = 10, \bar{c}_d = 0.1$		4.83425	4.54296	4.49522	4.50341	4.50555	4.50200	
(1,2)	Akavci [35]	5.3003	4.0906	3.6900	3.3952	3.3031	3.2626	
	Thai et al. [44]	5.2813	4.0781	3.6805	3.3938	3.2964	3.2514	
	Hosseini et al. [3]	5.2802	4.0773	3.6953	3.4492	3.3587	3.3094	
	Mantari et al. [36]	5.3039	4.1487	3.7677	3.4633	3.3484	3.2955	
	Present	$\bar{k}_w = \bar{k}_s = \bar{c}_d = 0$	5.30428	4.14891	3.76818	3.46376	3.34863	3.29565
		$\bar{k}_w = 10, \bar{k}_s = 0, \bar{c}_d = 0.1$	5.38275	4.26554	3.90401	3.62103	3.51478	3.46565
		$\bar{k}_w = 0, \bar{k}_s = 10, \bar{c}_d = 0.1$	6.67940	6.03846	5.88419	5.81358	5.78825	5.77233
$\bar{k}_w = 10, \bar{k}_s = 10, \bar{c}_d = 0.1$		6.74143	6.11832	5.97100	5.90714	5.88422	5.86923	
(1,3)	Akavci [35]	8.1179	6.2950	5.6614	5.1479	4.9921	4.9313	
	Thai et al. [44]	8.0749	6.2663	5.6390	5.1425	4.9758	4.9055	
	Hosseini et al. [3]	8.0710	6.2636	5.6695	5.2579	5.1045	5.0253	
	Mantari et al. [36]	8.1244	6.3814	5.7751	5.2484	5.0560	4.9747	
	Present	$\bar{k}_w = \bar{k}_s = \bar{c}_d = 0$	8.12516	6.38194	5.77596	5.24934	5.05661	4.97515
		$\bar{k}_w = 10, \bar{k}_s = 0, \bar{c}_d = 0.1$	8.17497	6.45589	5.86279	5.35193	5.16569	5.08687
		$\bar{k}_w = 0, \bar{k}_s = 10, \bar{c}_d = 0.1$	9.58143	8.41316	8.08122	7.86334	7.78824	7.75204
$\bar{k}_w = 10, \bar{k}_s = 10, \bar{c}_d = 0.1$		9.62310	8.46823	8.14203	7.93018	7.85721	7.82177	
(2,1)	Akavci [35]	10.1828	7.9209	7.1105	6.4181	6.2111	6.1355	
	Thai et al. [44]	10.1164	7.8762	7.0751	6.4074	6.1846	6.0954	
	Hosseini et al. [3]	9.7416	7.8711	7.1189	6.5749	5.9062	5.7518	
	Mantari et al. [36]	10.1907	8.0264	7.2479	6.5397	6.2856	6.1833	
	Present	$\bar{k}_w = \bar{k}_s = \bar{c}_d = 0$	10.19182	8.02721	7.24906	6.54102	6.28651	6.18403
		$\bar{k}_w = 10, \bar{k}_s = 0, \bar{c}_d = 0.1$	10.23084	8.08500	7.31724	6.62262	6.37363	6.27329
		$\bar{k}_w = 0, \bar{k}_s = 10, \bar{c}_d = 0.1$	11.69616	10.13547	9.65993	9.31233	9.19418	9.14170
$\bar{k}_w = 10, \bar{k}_s = 10, \bar{c}_d = 0.1$		11.72947	10.17994	9.70947	9.36749	9.25130	9.19949	

Table 9. Non-dimensional natural frequencies $\tilde{\omega} = (\omega a^2/h)\sqrt{\rho_c/E_c}$ for Al/Al₂O₃ FG rectangular plates on Visco-Winkler-Pasternak foundations ($b/a = 2, a/h = 10$).

Mode	Theory	p						
		0	1	2	5	8	10	
(1,1)	Akavci [35]	3.6542	2.7952	2.5376	2.3915	2.3418	2.3124	
	Thai et al. [44]	3.6518	2.7937	2.5364	2.3916	2.3411	2.3110	
	Hosseini et al. [3]	3.6518	2.7937	2.5386	2.3998	2.3504	2.3197	
	Mantari et al. [36]	3.6549	2.8365	2.5943	2.4398	2.3761	2.3398	
	Present	$\bar{k}_w = \bar{k}_s = \bar{c}_d = 0$	3.65486	2.83651	2.59442	2.43983	2.37599	2.33961
		$\bar{k}_w = 10, \bar{k}_s = 0, \bar{c}_d = 0.1$	3.77600	3.01640	2.80120	2.67192	2.61867	2.58757
		$\bar{k}_w = 0, \bar{k}_s = 10, \bar{c}_d = 0.1$	4.94508	4.58507	4.52571	4.53573	4.53665	4.53077
$\bar{k}_w = 10, \bar{k}_s = 10, \bar{c}_d = 0.1$		5.03519	4.69835	4.64720	4.66450	4.66813	4.66344	
(1,2)	Akavci [35]	5.7754	4.4231	4.0118	3.7682	3.6864	3.6403	
	Thai et al. [44]	5.7694	4.4192	4.0090	3.7682	3.6846	3.6368	
	Hosseini et al. [3]	5.7693	4.4192	4.0142	3.7881	3.7072	3.6580	
	Mantari et al. [36]	5.7769	4.4881	4.1008	3.8443	3.7401	3.6827	
	Present	$\bar{k}_w = \bar{k}_s = \bar{c}_d = 0$	5.77698	4.48818	4.10112	3.84448	3.74004	3.68252
		$\bar{k}_w = 10, \bar{k}_s = 0, \bar{c}_d = 0.1$	5.85372	4.60305	4.23389	3.99463	3.89754	3.84363
		$\bar{k}_w = 0, \bar{k}_s = 10, \bar{c}_d = 0.1$	7.13799	6.38008	6.21360	6.16032	6.13672	6.11716
$\bar{k}_w = 10, \bar{k}_s = 10, \bar{c}_d = 0.1$		7.20008	6.46117	6.30177	6.25482	6.23361	6.21512	
(1,3)	Akavci [35]	9.2029	7.0612	6.3959	5.9766	5.8388	5.7662	
	Thai et al. [44]	9.1880	7.0515	6.3886	5.9765	5.8341	5.7575	
	Hosseini et al. [3]	9.1876	7.0512	6.4015	6.0247	5.8887	5.8086	
	Mantari et al. [36]	9.2066	7.1643	6.5363	6.0976	5.9231	5.8315	
	Present	$\bar{k}_w = \bar{k}_s = \bar{c}_d = 0$	9.20678	7.16448	6.53682	6.09800	5.92308	5.83137
		$\bar{k}_w = 10, \bar{k}_s = 0, \bar{c}_d = 0.1$	9.25458	7.23620	6.62003	6.19285	6.02286	5.93351
		$\bar{k}_w = 0, \bar{k}_s = 10, \bar{c}_d = 0.1$	10.62513	9.17828	8.80991	8.61977	8.54454	8.49887
$\bar{k}_w = 10, \bar{k}_s = 10, \bar{c}_d = 0.1$		10.66630	9.23397	8.87138	8.68657	8.61339	8.56863	
(2,1)	Akavci [35]	11.8560	9.1093	8.2428	7.6738	7.4892	7.3965	
	Thai et al. [44]	11.8315	9.0933	8.2309	7.6731	7.4813	7.3821	
	Hosseini et al. [3]	11.8310	9.0928	8.2515	7.7505	7.5688	7.4639	
	Mantari et al. [36]	11.8616	9.2416	8.4222	7.8291	7.5963	7.4783	
	Present	$\bar{k}_w = \bar{k}_s = \bar{c}_d = 0$	11.86203	9.24189	8.42299	7.82973	7.59651	7.47829
		$\bar{k}_w = 10, \bar{k}_s = 0, \bar{c}_d = 0.1$	11.89892	9.29724	8.48733	7.90347	7.67423	7.55787
		$\bar{k}_w = 0, \bar{k}_s = 10, \bar{c}_d = 0.1$	13.30715	11.31242	10.77355	10.45683	10.33484	10.26714
$\bar{k}_w = 10, \bar{k}_s = 10, \bar{c}_d = 0.1$		13.33967	11.35714	10.82331	10.51139	10.39125	10.32437	

Table 10. Non-dimensional natural frequencies $\tilde{\omega} = (\omega a^2/h) \sqrt{\rho_c/E_c}$ for Al/Al₂O₃ FG rectangular plates resting on Visco-Winkler-Pasternak foundations ($b/a = 2, a/h = 20$).

Mode	Theory	p						
		0	1	2	5	8	10	
(1,1)	Akavci [35]	3.7129	2.8357	2.5774	2.4402	2.3924	2.3623	
	Thai et al. [44]	3.7123	2.8352	2.5771	2.4403	2.3923	2.3619	
	Hosseini et al. [3]	3.7123	2.8352	2.5777	2.4425	2.3948	2.3642	
	Mantari et al. [36]	3.7132	2.8777	2.6354	2.4892	2.4277	2.3908	
	Present	$\bar{k}_w = \bar{k}_s = \bar{c}_d = 0$	3.71313	2.87770	2.63557	2.48923	2.42750	2.39055
		$\bar{k}_w = 10, \bar{k}_s = 0, \bar{c}_d = 0.05$	3.83394	3.05727	2.84172	2.71973	2.66821	2.63648
		$\bar{k}_w = 0, \bar{k}_s = 10, \bar{c}_d = 0.05$	5.00322	4.62897	4.56905	4.58347	4.58523	4.57888
$\bar{k}_w = 10, \bar{k}_s = 10, \bar{c}_d = 0.05$		5.09349	4.74266	4.69098	4.71261	4.71708	4.71193	
(1,2)	Akavci [35]	5.9215	4.5238	4.1108	3.8883	3.8112	3.7632	
	Thai et al. [44]	5.9199	4.5228	4.1100	3.8884	3.8107	3.7622	
	Hosseini et al. [3]	5.9198	4.5228	4.1115	3.8939	3.8170	3.7681	
	Mantari et al. [36]	5.9220	4.5909	4.2032	3.9665	3.8672	3.8084	
	Present	$\bar{k}_w = \bar{k}_s = \bar{c}_d = 0$	5.92192	4.59085	4.20342	3.96649	3.86700	3.80806
		$\bar{k}_w = 10, \bar{k}_s = 0, \bar{c}_d = 0.05$	5.99822	4.70524	4.33538	4.11474	4.02212	3.96672
		$\bar{k}_w = 0, \bar{k}_s = 10, \bar{c}_d = 0.05$	7.28089	6.48489	6.31643	6.27436	6.25285	6.23193
$\bar{k}_w = 10, \bar{k}_s = 10, \bar{c}_d = 0.05$		7.34305	6.56631	6.40495	6.36905	6.34989	6.33007	
(1,3)	Akavci [35]	9.5711	7.3159	6.6453	6.2759	6.1488	6.0715	
	Thai et al. [44]	9.5669	7.3132	6.6433	6.2760	6.1476	6.0690	
	Hosseini et al. [3]	9.5668	7.3132	6.6471	6.2903	6.1639	6.0843	
	Mantari et al. [36]	9.5723	7.4242	6.7942	6.4023	6.2391	6.1440	
	Present	$\bar{k}_w = \bar{k}_s = \bar{c}_d = 0$	9.57223	7.42418	6.79463	6.40232	6.23878	6.14351
		$\bar{k}_w = 10, \bar{k}_s = 0, \bar{c}_d = 0.05$	9.61945	7.49521	6.87676	6.49490	6.33580	6.24279
		$\bar{k}_w = 0, \bar{k}_s = 10, \bar{c}_d = 0.05$	10.98422	9.43713	9.06263	8.90094	8.83088	8.78146
$\bar{k}_w = 10, \bar{k}_s = 10, \bar{c}_d = 0.05$		11.02533	9.49302	9.124280	8.96765	8.89955	8.85106	
(2,1)	Akavci [35]	12.4633	9.5307	8.6542	8.1634	7.9954	7.8950	
	Thai et al. [44]	12.4562	9.5261	8.6509	8.1636	7.9934	7.8909	
	Hosseini et al. [3]	12.4560	9.5261	8.6572	8.1875	8.0207	7.9166	
	Mantari et al. [36]	12.4652	9.6715	8.8478	8.3279	8.1127	7.9888	
	Present	$\bar{k}_w = \bar{k}_s = \bar{c}_d = 0$	12.46522	9.67154	8.84835	8.32803	8.11232	7.98825
		$\bar{k}_w = 10, \bar{k}_s = 0, \bar{c}_d = 0.05$	12.50143	9.72605	8.91143	8.39926	8.18701	8.06469
		$\bar{k}_w = 0, \bar{k}_s = 10, \bar{c}_d = 0.05$	13.89984	11.73763	11.18768	10.91733	10.80357	10.72952
$\bar{k}_w = 10, \bar{k}_s = 10, \bar{c}_d = 0.05$		13.93224	11.78246	11.23750	10.97160	10.85959	10.78637	

Tables 11–14 present the non-dimensional fundamental frequencies for Aluminum-Alumina (Al/Al₂O₃) FG rectangular plates resting on visco-Pasternak foundations ($\bar{k}_w = 0, \bar{k}_s = 100$). Several values of the FG power-law index p , aspect ratio a/b , and side-to-thickness ratio a/h are considered. In fact, there is no foundation in Table 11, and the inclusion of one-by-one elastic foundation is made in Tables 12–14. In such tables, the inclusion of the third-parameter coefficient \bar{c}_d is also discussed. The non-dimensional frequency and the non-dimensional third coefficient of the viscoelastic foundations are utilized as

$$\tilde{\omega} = \frac{\omega a^2}{h} \sqrt{\frac{\rho_m}{E_m}}, \bar{c}_d = c_d h \sqrt{\frac{h}{\rho_m D_m}}, \tag{39}$$

and the other non-dimensional coefficients of the two-parameter foundations are given in Equation (37). In the absence of the third coefficient of the viscoelastic foundations \bar{c}_d , the present frequencies are compared with the HSDTs proposed by Thai and Choi [38], Akavci [35], and a quasi-3D hybrid type HSDT by Mantari et al. [36]

Table 11. Non-dimensional fundamental frequencies $\check{\omega} = (\omega a^2/h)\sqrt{\rho_m/E_m}$ for Al/Al₂O₃ FG rectangular plates ($\bar{k}_w = \bar{k}_s = \bar{c}_d = 0$).

<i>alb</i>	<i>a/h</i>	<i>p</i>	Akavci [35]	Thai and Choi [38]	Mantari et al. [36]	Present	
0.5	5	1	5.2122	5.2016	5.2875	5.28772	
		5	4.3763	4.3757	4.4648	4.46520	
		10	4.2153	4.2058	4.2611	4.26116	
	10	1	5.4918	5.4887	5.5728	5.57286	
		5	4.6986	4.6987	4.7934	4.79350	
		10	4.5432	4.5404	4.5969	4.59661	
	20	1	5.5712	5.5704	5.6538	5.65379	
		5	4.7943	4.7943	4.8906	4.89057	
		10	4.6411	4.6404	4.6971	4.69669	
	1	5	1	8.0368	8.0122	8.1509	8.15131
			5	6.6705	6.6678	6.8043	6.80521
			10	6.4099	6.3879	6.4746	6.47492
10		1	8.6899	8.6824	8.8178	8.81788	
		5	7.4033	7.4034	7.5529	7.55319	
		10	7.1521	7.1453	7.2353	7.23501	
20		1	8.8879	8.8859	9.0196	9.01959	
		5	7.6393	7.6394	7.7929	7.79291	
		10	7.3934	7.3916	7.4823	7.48166	
2		5	1	17.8289	17.7148	18.0607	18.06273
			5	14.3625	14.3312	14.6274	14.63068
			10	13.7120	13.6095	13.8083	13.81014
	10	1	20.8487	20.8063	21.1501	21.15090	
		5	17.5051	17.5028	17.8593	17.86082	
		10	16.8613	16.8232	17.0445	17.04463	
	20	1	21.9670	21.9548	22.2914	22.29144	
		5	18.7946	18.7950	19.1737	19.17401	
		10	18.1727	18.1616	18.3877	18.38645	

Table 12. Non-dimensional fundamental frequencies $\tilde{\omega} = (\omega a^2/h)\sqrt{\rho_m/E_m}$ for Al/Al₂O₃ FG rectangular plates resting on visco-Winkler foundations ($\bar{k}_w = 100, \bar{k}_s = 0$).

<i>a/b</i>	<i>a/h</i>	<i>p</i>	Akavci [35]	Thai and Choi [38]	Mantari et al. [36]	Present	
						$\bar{c}_d = 0$	$\bar{c}_d = 0.25$
0.5	5	1	5.8746	5.8654	5.9257	5.92588	5.92620
		5	5.2360	5.2355	5.2934	5.29366	5.29417
		10	5.1288	5.1212	5.1467	5.14660	5.14722
	10	1	6.1393	6.1366	6.2077	6.20770	6.20801
		5	5.5276	5.5277	5.6038	5.60384	5.60430
		10	5.4199	5.4176	5.4596	5.45931	5.45987
	20	1	6.2152	6.2144	6.2883	6.28824	6.28829
		5	5.6156	5.6157	5.6969	5.69685	5.69692
		10	5.5087	5.5080	5.5545	5.55415	5.55422
1	5	1	8.4748	8.4517	8.5671	8.56752	8.56801
		5	7.2560	7.2534	7.3618	7.36260	7.36336
		10	7.0373	7.0175	7.0758	7.07594	7.07683
	10	1	9.1107	9.1035	9.2282	9.22829	9.22876
		5	7.9520	7.9521	8.0866	8.08681	8.08751
		10	7.7356	7.7293	7.8067	7.80636	7.80720
	20	1	9.3044	9.3025	9.4292	9.42918	9.42925
		5	8.1789	8.1790	8.3212	8.32122	8.32132
		10	7.9658	7.9640	8.0468	8.04617	8.04629
2	5	1	18.0231	17.9108	18.2385	18.24050	18.24161
		5	14.6363	14.6057	14.8810	14.88418	14.88578
		10	14.0098	13.9101	14.0861	14.08780	14.08965
	10	1	21.0241	20.9821	21.3187	21.31945	21.32062
		5	17.7396	17.7373	18.0843	18.08585	18.08761
		10	17.1126	17.0751	17.2873	17.28741	17.28949
	20	1	22.1378	22.1257	22.4585	22.45857	22.45967
		5	19.0187	19.0192	19.3921	19.39248	19.39408
		10	18.4115	18.4005	18.6222	18.62087	18.62278

It can be seen from Tables 11–14 that the present frequencies are in excellent agreement with the corresponding results of Mantari et al. [36] and slightly more than those of Thai and Choi [38] and Akavci [35]. The frequencies increase as both *a/h* and *a/b* increase and as *p* decreases in case of neglecting the foundation medium. The frequency when *a/b* = 2 is more than twice of this when *a/b* = 1.

Table 13. Non-dimensional fundamental frequencies $\tilde{\omega} = (\omega a^2/h)\sqrt{\rho_m/E_m}$ for Al/Al₂O₃ FG rectangular plates resting on visco–Pasternak foundations ($\bar{k}_w = 0, \bar{k}_s = 100$).

<i>a/b</i>	<i>a/h</i>	<i>p</i>	Akavci [35]	Thai and Choi [38]	Mantari et al. [36]	Present	
						$\bar{c}_d = 0$	$\bar{c}_d = 0.25$
0.5	5	1	10.8489	10.8450	10.7649	10.76493	10.76552
		5	10.9925	10.9919	10.9106	10.91023	10.91134
		10	11.0818	11.0793	10.9611	10.96027	10.96164
	10	1	11.0940	11.0926	11.1042	11.10417	11.10472
		5	11.2538	11.2538	11.2645	11.26443	11.26537
		10	11.3313	11.3302	11.3190	11.31873	11.31989
	20	1	11.1660	11.1656	11.1999	11.19984	11.20017
		5	11.3343	11.3343	11.3680	11.36794	11.36849
		10	11.4093	11.4090	11.4236	11.42342	11.42390
1	5	1	14.3923	14.3818	14.2406	14.24088	14.24170
		5	14.3071	14.3052	14.1562	14.15569	14.15721
		10	14.3829	14.3759	14.1600	14.15860	14.16046
	10	1	14.9443	14.9401	14.9631	14.96319	14.96395
		5	14.8693	14.8692	14.8895	14.88945	14.89075
		10	14.9193	14.9162	14.8957	14.89520	14.89681
	20	1	15.1189	15.1177	15.1825	15.18244	15.18316
		5	15.0607	15.0607	15.1251	15.12506	15.12623
		10	15.1056	15.1047	15.1330	15.13257	15.13403
2	5	1	25.6912	25.6294	25.2563	25.25781	25.25932
		5	24.3625	24.3453	23.8994	23.89854	23.90119
		10	24.3109	24.2696	23.6297	23.62625	23.62944
	10	1	28.2316	28.2023	28.2878	28.28833	28.28988
		5	26.7223	26.7201	26.7859	26.78627	26.78890
		10	26.5586	26.5362	26.4775	26.47653	26.47974
	20	1	29.2272	29.2181	29.4271	29.42715	29.42860
		5	27.7770	27.7772	27.9891	27.98915	27.99147
		10	27.5919	27.5847	27.6803	27.67920	27.68203

In each table, in addition to the examination of the aspect ratios *a/b*, thickness ratios *a/h*, and the FG power-law index *p*, we discussed several combinations of the foundation parameters \bar{k}_w and \bar{k}_s . Furthermore, different values of the third damping coefficient \bar{c}_d are considered. The results show that the three Visco-Winkler-Pasternak foundation parameters have effects of increasing the non-dimensional frequencies. The Pasternak parameter \bar{k}_s has more of an effect on increasing the frequencies than the Winkler parameter \bar{k}_w . However, the damping parameter \bar{c}_d has a little and sensitive effect on increasing the frequencies. It is interesting to discuss the effect of the FG power-law index *p* on the non-dimensional frequencies. As shown in Table 11, the frequency parameter $\tilde{\omega}$ decreases with the increase in *p* and this is irrespective of the values of *a/h* and *a/b*. Additionally, it is observed in Table 12 that if a plate is just rested on Winkler’s foundation or visco-Winkler foundations, the increase of the FG power-law index decreases the non-dimensional frequency. However, this situation is inversed if the plate is rested on Pasternak’s foundation regardless of the absence (Table 13) or presence (Table 14) of Winkler’s foundation or visco-Winkler foundations.

Table 14. Non-dimensional fundamental frequencies $\tilde{\omega} = (\omega a^2/h) \sqrt{\rho_m/E_m}$ for Al/Al₂O₃ FG rectangular plates resting on Visco-Winkler-Pasternak foundations ($\bar{k}_w = 100, \bar{k}_s = 100$).

<i>a/b</i>	<i>a/h</i>	<i>p</i>	Akavci [35]	Thai and Choi [38]	Mantari et al. [36]	Present	
						$\bar{c}_d = 0$	$\bar{c}_d = 0.25$
0.5	5	1	11.1817	11.1780	11.0894	11.08946	11.09007
		5	11.3598	11.3593	11.2700	11.26956	11.27071
		10	11.4581	11.4558	11.3285	11.32767	11.32909
	10	1	11.4284	11.4270	11.4358	11.43582	11.43638
		5	11.6243	11.6243	11.6322	11.63214	11.63311
		10	11.7103	11.7093	11.6957	11.69536	11.69657
	20	1	11.5008	11.5005	11.5331	11.53311	11.53346
		5	11.7054	11.7054	11.7374	11.73738	11.73796
		10	11.7888	11.7886	11.8021	11.80186	11.80257
1	5	1	14.6407	14.6305	14.4792	14.47947	14.48030
		5	14.5862	14.5843	14.4258	14.42519	14.42675
		10	14.6702	14.6636	14.4366	14.43508	14.43698
	10	1	15.1927	15.1887	15.2084	15.20848	15.20924
		5	15.1498	15.1497	15.1669	15.16678	15.16811
		10	15.2075	15.2045	15.1810	15.18053	15.18217
	20	1	15.3674	15.3663	15.4293	15.42927	15.43000
		5	15.3414	15.3414	15.4039	15.40390	15.40509
		10	15.3938	15.3929	15.4198	15.41946	15.42094
2	5	1	25.8251	25.7640	25.3782	25.37974	25.38125
		5	24.5206	24.5036	24.0450	24.04408	24.04674
		10	24.4759	24.4352	23.7803	23.77672	23.77992
	10	1	28.3613	28.3322	28.4137	28.41429	28.41586
		5	26.8763	26.8741	26.9360	26.93632	26.93896
		10	26.7186	26.6964	26.6338	26.63282	26.63605
	20	1	29.3557	29.3467	29.5539	29.55394	29.55539
		5	27.9292	27.9294	28.1392	28.13924	28.14156
		10	27.7497	27.7426	27.8366	27.83544	27.83829

Table 15 presents the non-dimensional fundamental frequencies for Al/Al₂O₃ FG rectangular plates resting on viscoelastic foundations with $h/a = 0.15$ and several values of a/b . The non-dimensional frequency and the non-dimensional viscoelastic foundation coefficients are utilized as

Table 15. Non-dimensional fundamental frequencies for Al/Al₂O₃ FG rectangular plates ($h/a = 0.15$).

(k_w, k_s)	a/b	Theory	p			
			0	1	5	∞
(0,0)	0.5	Akavci [35]	0.08018	0.06148	0.05215	0.04081
		Hosseini et al. [3]	0.08006	0.06335	0.05379	0.04100
		Mantari et al. [36]	0.08021	0.06238	0.05321	0.04083
		Present $\bar{c}_d = 0$	0.080209	0.062382	0.053210	0.040825
	1	Akavci [35]	0.12508	0.09613	0.08089	0.06366
		Hosseini et al. [3]	0.12480	0.09644	0.08027	0.06335
		Mantari et al. [36]	0.12514	0.09753	0.08253	0.06370
		Present $\bar{c}_d = 0$	0.12514	0.09753	0.08253	0.063696
	2	Akavci [35]	0.28659	0.22189	0.18232	0.14587
		Hosseini et al. [3]	0.28513	0.20592	0.16315	0.14591
		Mantari et al. [36]	0.28682	0.22498	0.18592	0.14600
		Present $\bar{c}_d = 0$	0.286844	0.224999	0.185947	0.146000
(100,10)	0.5	Baferani et al. [45]	0.12869	0.10498	0.09227	—
		Akavci [35]	0.12876	0.10388	0.09098	0.06554
		Hosseini et al. [3]	0.12870	0.10519	0.09223	0.06591
		Mantari et al. [36]	0.12804	0.10388	0.09118	0.06517
		Present $\bar{c}_d = 0$	0.128037	0.103883	0.091179	0.065169
		Present $\bar{c}_d = 0.5$	0.128140	0.103981	0.091284	0.065243
	1	Baferani et al. [45]	0.17020	0.13854	0.12077	—
		Akavci [35]	0.17039	0.13592	0.11774	0.08673
		Hosseini et al. [3]	0.17020	0.13652	0.11786	0.08663
		Mantari et al. [36]	0.16931	0.13610	0.11825	0.08618
		Present $\bar{c}_d = 0$	0.169312	0.136102	0.118253	0.086178
		Present $\bar{c}_d = 0.5$	0.169454	0.136236	0.118398	0.086279
2	Baferani et al. [45]	0.31449	0.26966	0.22932	—	
	Akavci [35]	0.32889	0.25901	0.21785	0.16741	
	Hosseini et al. [3]	0.32768	0.24674	0.20359	0.16773	
	Mantari et al. [36]	0.32670	0.25992	0.21953	0.16630	
	Present $\bar{c}_d = 0$	0.326723	0.259934	0.219551	0.166298	
	Present $\bar{c}_d = 0.5$	0.327020	0.260213	0.219848	0.166511	

$$\tilde{\omega} = \omega h \sqrt{\frac{\rho_c}{E_c}}, \bar{c}_d = c_d h \sqrt{\frac{h}{\rho_c D_c}}, \bar{k}_w = \frac{a^4}{D_c} k_w, \bar{k}_s = \frac{a^2}{D_c} k_s, \bar{D}_c = \frac{h^3}{12(1-\nu^2)} \frac{p(p^2+3p+8)E_m+3(p^2+p+2)E_c}{(1+p)(2+p)(3+p)} \tag{40}$$

It is to be noted that when $p \rightarrow 0$ (ceramic plate), \bar{D}_c will tends to D_c while when $p \rightarrow \infty$ (metal plate) \bar{D}_c will tends to D_m .

The present frequencies are compared with the corresponding ones of the FSDT of Hosseini-Hashemi et al. [3], the HSDTs proposed by Akavci [35] and Baferani et al. [45], and a quasi-3D hybrid type HSDT by Mantari et al. [36] It can be seen from this table that the present results are identical to those proposed by Mantari et al. [36], close to the ones of Akavci [38] and Mantari et al. [36], and slightly more than those of Baferani et al. [45] Once again, the frequencies increase with the inclusion of the damping coefficient \bar{c}_d .

Table 16 presents the non-dimensional fundamental frequencies for Aluminum-Zirconia (Al/ZrO₂) FG rectangular plates ($a/b = 1.5$) resting on viscoelastic foundations with several values of the side-to-thickness ratio a/h . The non-dimensional frequency and the non-dimensional viscoelastic foundation coefficients are utilized as given in Equation (40). The present solution is compared with the corresponding ones of the theories presented in Table 15. In general, the frequencies are slightly decreasing as the FG power-law index p increases while they rapidly increase as the side-to-thickness ratio a/h increases. Furthermore,

the inclusion of the viscoelastic foundations increases the values of the frequency parameter. Once again, the present results are identical to those proposed by Mantari et al. [36] for free pleats or plates resting on elastic foundations. In the case of $\bar{k}_w = \bar{k}_s = 0$, the present frequencies are slightly greater than those proposed by Akavci [38] and Hosseini et al. [3]. However, in the case of $\bar{k}_w = 250, \bar{k}_s = 25$, the present frequencies are slightly smaller than those proposed by Akavci [38] and Hosseini et al. [3], especially when $a/h \geq 10$. In the case of the viscoelastic coefficients, the frequencies increase with the inclusion of the damping coefficient \bar{c}_d .

Table 16. Non-dimensional fundamental frequencies $\tilde{\omega} = \omega h \sqrt{\rho_c/E_c}$ for Al/ZrO₂ FG rectangular plates ($a/b = 1.5$).

(\bar{k}_w, \bar{k}_s)	a/h	Theory	p			
			0	1	5	∞
(0,0)	20	Akavci [35]	0.02393	0.02202	0.02244	0.02056
		Hosseini et al. [3]	0.02392	0.02156	0.02180	0.02046
		Mantari et al. [36]	0.02393	0.02217	0.02260	0.02057
		Present $\bar{c}_d = 0$	0.023931	0.022174	0.022597	0.02056
	10	Akavci [35]	0.09203	0.08489	0.08576	0.07908
		Hosseini et al. [3]	0.09188	0.08155	0.08171	0.07895
		Mantari et al. [36]	0.09207	0.08549	0.08638	0.07911
		Present $\bar{c}_d = 0$	0.092068	0.085493	0.086386	0.079111
	5	Akavci [35]	0.32471	0.30152	0.31860	0.27902
		Hosseini et al. [3]	0.32284	0.29399	0.29099	0.27788
		Mantari et al. [36]	0.32498	0.30349	0.29990	0.27925
		Present $\bar{c}_d = 0$	0.325006	0.303514	0.299939	0.279268
(250,25)	20	Baferani et al. [45]	0.03421	0.03249	0.03314	—
		Akavci [35]	0.03422	0.03213	0.03277	0.02940
		Hosseini et al. [3]	0.03421	0.03184	0.03235	0.02937
		Mantari et al. [36]	0.03417	0.03220	0.03283	0.02936
		Present $\bar{c}_d = 0$	0.034169	0.032200	0.032834	0.029361
		Present $\bar{c}_d = 0.5$	0.034272	0.032213	0.032848	0.029395
	10	Baferani et al. [45]	0.13365	0.12749	0.12950	—
		Akavci [35]	0.13375	0.12585	0.12778	0.11492
		Hosseini et al. [3]	0.13365	0.12381	0.12533	0.11484
		Mantari et al. [36]	0.13302	0.12557	0.12755	0.11430
		Present $\bar{c}_d = 0$	0.133019	0.125569	0.127554	0.114299
		Present $\bar{c}_d = 0.5$	0.133127	0.125707	0.127731	0.114495
5	Baferani et al. [45]	0.43246	0.46406	0.44824	—	
	Akavci [35]	0.50044	0.47298	0.47637	0.43000	
	Hosseini et al. [3]	0.49945	0.46997	0.47400	0.43001	
	Mantari et al. [36]	0.48945	0.46401	0.46838	0.42057	
	Present $\bar{c}_d = 0$	0.489466	0.464028	0.468392	0.420583	
	Present $\bar{c}_d = 0.5$	0.489910	0.464595	0.469153	0.421389	

3.5. Parametric Studies

The above two sections are concerned with verifying the accuracy of the present model with the corresponding ones available in the literature. The present parametric studies are carried out to investigate the influences of the FG power-law index p , aspect ratio a/b , thickness ratio a/h , and the two foundation parameters \bar{k}_w and \bar{k}_s on the natural frequency of Al/Al₂O₃ and Al/ZrO₂ plates. In addition, the effect of the damping parameter \bar{c}_d is taken into consideration in most cases.

The variations of non-dimensional natural frequencies for Aluminum-Alumina (Al/Al₂O₃) FG rectangular plates concerning different parameters are presented in Tables 17 and 18. The thickness and aspect ratios and the first mode number are fixed as $i = 1, h/a = 0.2$, and $b/a = 0.5$, respectively. The effects of the FG power-law index p , the second mode number j ,

and the Visco-Winkler-Pasternak foundations $\bar{k}_w, \bar{k}_s,$ and \bar{c}_d . The frequencies increase as all parameters increase, except the FG power-law index p for which the frequencies decrease.

Table 17. Non-dimensional fundamental frequencies $\tilde{\omega} = \omega h \sqrt{\rho_c/E_c}$ for Al/Al₂O₃ FG rectangular plates ($h/a = 0.2, b/a = 0.5$).

Mode	\bar{k}_s	\bar{k}_w	\bar{c}_d	p				
				0	1	2	5	∞
(1,1)	0	0	0	0.46607	0.36775	0.33164	0.29787	0.23722
			0	0.46741	0.36892	0.33283	0.29905	0.23790
		10	1	0.46916	0.37056	0.33448	0.30070	0.23917
			2	0.47462	0.37569	0.33960	0.30576	0.24314
		100	0	0.47923	0.37925	0.34336	0.30943	0.24392
			1	0.48103	0.38094	0.34506	0.31114	0.24521
	10	0	2	0.48661	0.38621	0.35034	0.31638	0.24928
			0	0.52750	0.42118	0.38575	0.35094	0.26849
		10	1	0.52947	0.42304	0.38766	0.35288	0.26990
			2	0.53558	0.42886	0.39358	0.35885	0.27436
		100	0	0.52866	0.42218	0.38676	0.35193	0.26908
			1	0.53063	0.42405	0.38868	0.35387	0.27050
2	0.53675	0.42988	0.39461	0.35986	0.27496			
0	0	0.53900	0.43112	0.39573	0.36066	0.24392		
1	0.54101	0.43302	0.39769	0.36265	0.24521			
2	0.54724	0.43897	0.40376	0.36879	0.24928			

Table 18. Non-dimensional natural frequencies $\tilde{\omega} = \omega h \sqrt{\rho_c/E_c}$ for Al/Al₂O₃ FG rectangular plates ($h/a = 0.2, b/a = 0.5$).

Mode	\bar{k}_s	\bar{k}_w	\bar{c}_d	p				
				0	1	2	5	∞
(1,2)	0	0	0	1.17023	0.93832	0.83770	0.72561	0.59563
			0	1.17072	0.93873	0.83813	0.72607	0.59588
		10	1	1.17499	0.94280	0.84212	0.72977	0.59895
			2	1.18832	0.95560	0.85469	0.74137	0.60870
		100	0	1.17508	0.94244	0.84202	0.73020	0.59810
			1	1.17935	0.94652	0.84602	0.73391	0.60117
	10	0	2	1.19270	0.95933	0.85861	0.74557	0.61093
			0	1.24726	1.00366	0.90580	0.79747	0.63484
		10	1	1.25160	1.00781	0.90995	0.80143	0.63796
			2	1.26515	1.02085	0.92301	0.81384	0.64785
		100	0	1.24769	1.00402	0.90618	0.79787	0.63506
			1	1.25204	1.00818	0.91033	0.80183	0.63818
2	1.26558	1.02122	0.92339	0.81424	0.64807			
0	0	1.25158	1.00731	0.90959	0.80144	0.63704		
1	1.25593	1.01147	0.91375	0.80541	0.64016			
2	1.26948	1.02452	0.92683	0.81787	0.65006			

Table 18. Cont.

Mode	\bar{k}_s	\bar{k}_w	\bar{c}_d	p				
				0	1	2	5	∞
(1,3)	0	0	0	1.95174	1.58204	1.40727	1.19641	0.99341
			0	1.95203	1.58228	1.40752	1.19669	0.99356
		10	1	1.95889	1.58883	1.41381	1.20228	0.99849
			2	1.98029	1.60940	1.43361	1.21989	1.01411
		100	0	1.95461	1.58442	1.40979	1.19918	0.99487
			1	1.96146	1.59097	1.41607	1.20477	0.99979
	10	0	0	2.04872	1.66250	1.49197	1.28918	1.04277
			1	2.05515	1.66863	1.49797	1.29470	1.04739
		10	2	2.07508	1.68772	1.51677	1.31206	1.06190
			0	2.04897	1.66271	1.49218	1.28941	1.04290
		100	1	2.05539	1.66883	1.49818	1.29494	1.04751
			2	2.07532	1.68792	1.51698	1.31230	1.06202
100	0	0	2.05118	1.66453	1.49410	1.29150	1.04402	
		1	2.05759	1.67064	1.50009	1.29702	1.04863	
	2	2.07747	1.68970	1.51886	1.31437	1.06311		

4. Conclusions

In the present study, a refined quasi-3D elasticity theory is presented for natural vibration analysis of homogeneous and FG plates resting on Visco-Winkler-Pasternak foundations. The governing equations of motion are derived due to Hamilton’s principle. The closed-form solutions are obtained for different types of rectangular plates. A validation study is performed to verify the accuracy of the present frequencies. Furthermore, a parametric study is carried out to investigate the effects of various parameters on the natural frequencies of FG plates. Such parameters are the FG power-law index, aspect and thickness ratios, and foundation parameters, especially the inclusion of the third damping parameter. The following points can be outlined from the present study:

- The quasi-3D theory satisfies both the zero transverse and normal shear stress conditions on the plate surfaces and does not require any shear correction factor;
- Compared to other theories in the literature, the present quasi-3D theory produces accurate results for both thin and thick FG plates;
- One of the important notes is that Pasternak’s parameter has a greater effect on increasing the non-dimensional frequency than both the Winkler’s and visco-Winkler parameters;
- In general, in the inclusion of the viscoelastic foundation, increasing the value of Winkler, Pasternak, and damping coefficients causes an increase in the natural frequencies of FG plates;
- The FG power-law index affects reducing the non-dimensional frequencies of FG plates on visco-Winkler-Pasternak foundations.

Author Contributions: Conceptualization, A.M.Z. and M.A.A.; data curation, M.A.A.; funding acquisition, M.A.A.; investigation, A.M.Z.; methodology, A.M.Z.; project administration, A.M.Z.; resources, M.A.A.; software, M.A.A. and A.M.Z.; supervision, A.M.Z.; validation, A.M.Z.; visualization, A.M.Z.; writing—original draft preparation, M.A.A.; writing—review and editing, M.A.A. and A.M.Z. All authors have read and agreed to the published version of the manuscript.

Funding: The authors extend their appreciation to the Deputyship for Research & Innovation, Ministry of Education in Saudi Arabia for funding this research work through the project number (IFPHI-198-135-2020) and King Abdulaziz University, DSR, Jeddah, Saudi Arabia.

Data Availability Statement: Not applicable.

Acknowledgments: This research work was funded by Institutional Fund Projects under grant no. (IFPHI-198-135-2020). Therefore, the authors gratefully acknowledge technical and financial support from the Ministry of Education and King Abdulaziz University, DSR, Jeddah, Saudi Arabia.

Conflicts of Interest: The authors declare no conflict of interest.

References

- Koizumi, M. The concept of FGM ceramic transactions. *Funct. Gradient Mater.* **1993**, *34*, 3–10.
- Koizumi, M. FGM activities in Japan. *Compos. Part B Eng.* **1997**, *28*, 1–4. [[CrossRef](#)]
- Hosseini-Hashemi, S.; Taher, H.; Akhavan, H.; Omid, M. Free vibration of functionally graded rectangular plates using first-order shear deformation plate theory. *Appl. Math. Model.* **2010**, *34*, 1276–1291. [[CrossRef](#)]
- Pandey, S.; Pradyumna, S. Free vibration of functionally graded sandwich plates in thermal environment using a layerwise theory. *Europ. J. Mech.-A Solids* **2015**, *51*, 55–66. [[CrossRef](#)]
- Zenkour, A.M. Free vibration of a microbeam resting on Pasternak's foundation via the Green–Naghdi thermoelasticity theory without energy dissipation. *J. Low Freq. Noise Vib. Act. Control* **2016**, *35*, 303–311. [[CrossRef](#)]
- Benferhat, R.; Daouadji, T.; Mansour, M. Free vibration analysis of FG plates resting on an elastic foundation and based on the neutral surface concept using higher-order shear deformation theory. *Comptes Rendus Mécanique* **2016**, *344*, 631–641. [[CrossRef](#)]
- Zaoui, F.; Tounsi, A.; Ouinas, D. Free vibration of functionally graded plates resting on elastic foundations based on quasi-3D hybrid-type higher order shear deformation theory. *Smart Struct. Syst.* **2017**, *20*, 509–524.
- Zenkour, A.M.; Radwan, A.F. Free vibration analysis of multilayered composite and soft core sandwich plates resting on Winkler-Pasternak foundations. *J. Sand. Struct. Mater.* **2018**, *20*, 169–190. [[CrossRef](#)]
- Wang, Y.; Zeng, R.; Safarpour, M. Vibration analysis of FG-GPLRC annular plate in a thermal environment. *Mech. Based Des. Struct. Mach.* **2022**, *50*, 352–370. [[CrossRef](#)]
- Sobhy, M.; Zenkour, A.M. Vibration analysis of functionally graded graphene platelet-reinforced composite doubly-curved shallow shells on elastic foundations. *Steel Compos. Struct.* **2019**, *33*, 195–208.
- Kumar, V.; Singh, S.; Saran, V.; Harsha, V. An analytical framework for rectangular FGM tapered plate resting on the elastic foundation. *Mater. Today Proc.* **2020**, *28*, 1719–1726. [[CrossRef](#)]
- Liu, J.; Deng, X.; Wang, Q.; Zhong, R.; Xiong, R.; Zhao, J. A unified modeling method for dynamic analysis of GPL-reinforced FGP plate resting on Winkler-Pasternak foundation with elastic boundary conditions. *Compos. Struct.* **2020**, *244*, 112217. [[CrossRef](#)]
- Arefi, M.; Kiani, M.; Zenkour, A.M. Size-dependent free vibration analysis of a three-layered exponentially graded nano-/micro-plate with piezomagnetic face sheets resting on Pasternak's foundation via MCST. *J. Sand. Struct. Mater.* **2020**, *22*, 55–86. [[CrossRef](#)]
- Tran, T.; Nguyen, P.; Pham, Q. Vibration analysis of FGM plates in thermal environment resting on elastic foundation using ES-MITC3 element and prediction of ANN. *Case Stud. Therm. Eng.* **2021**, *24*, 100852. [[CrossRef](#)]
- Li, H.; Pang, F.; Chen, H.; Du, Y. Vibration analysis of functionally graded porous cylindrical shell with arbitrary boundary restraints by using a semi analytical method. *Compos. Part B Eng.* **2019**, *164*, 249–264. [[CrossRef](#)]
- Li, H.; Pang, F.; Du, Y.; Gao, C. Free vibration analysis of uniform and stepped functionally graded circular cylindrical shells. *Steel Compos. Struct.* **2019**, *33*, 163–180. [[CrossRef](#)]
- Radaković, A.; Čukanović, D.; Bogdanović, G.; Blagojević, M.; Stojanović, B.; Dragović, D.; Manić, N. Thermal buckling and free vibration analysis of functionally graded plate resting on an elastic foundation according to high order shear deformation theory based on eew shape function. *Appl. Sci.* **2020**, *10*, 4190. [[CrossRef](#)]
- Li, H.; Wang, W.; Yao, L. Analysis of the vibration behaviors of rotating composite nano-annular plates based on nonlocal theory and different plate theories. *Appl. Sci.* **2022**, *12*, 230. [[CrossRef](#)]
- Nguyen, P.; Pham, Q.; Tran, T.; Thoi, T. Effects of partially supported elastic foundation on free vibration of FGP plates using ES-MITC3 elements. *Ain Shams Eng. J.* **2021**, *13*, 101615.
- Tran, T.T.; Tran, V.K.; Pham, Q.-H.; Zenkour, A.M. Extended four-unknown higher-order shear deformation nonlocal theory for bending, buckling and free vibration of functionally graded porous nanoshell resting on elastic foundation. *Compos. Struct.* **2021**, *264*, 113737. [[CrossRef](#)]
- Zenkour, A.M.; El-Shahrany, H.D. Forced vibration of a magnetoelastic laminated composite beam on Pasternak's foundation. *J. Comput. Appl. Mech.* **2021**, *52*, 478–497.
- Zenkour, A.M. Vibration analysis of generalized thermoelastic microbeams resting on visco-Pasternak's foundations. *Adv. Aircr. Spacecr. Sci.* **2017**, *4*, 269–280. [[CrossRef](#)]
- Arefi, M.; Zenkour, A.M. Size-dependent free vibration and dynamic analyses of piezo-electro-magnetic sandwich nanoplates resting on viscoelastic foundation. *Appl. Phys. B* **2017**, *521*, 188–197. [[CrossRef](#)]
- Arefi, M.; Zenkour, A.M. Vibration and bending analyses of magneto-electro-thermo-elastic sandwich microplates resting on viscoelastic foundation. *Appl. Phys. A* **2017**, *123*, 550. [[CrossRef](#)]
- Zenkour, A.M.; El-Shahrany, H.D. Hygrothermal forced vibration of a viscoelastic laminated plate with magnetostrictive actuators resting on viscoelastic foundations. *Int. J. Mech. Mater. Des.* **2021**, *17*, 301–320. [[CrossRef](#)]

26. Zenkour, A.M.; El-Shahrany, H.D. Controlled motion of viscoelastic fiber-reinforced magnetostrictive sandwich plates resting on visco-Pasternak foundation. *Mech. Adv. Mater. Struct.* **2022**, *2020*, 1–10. [[CrossRef](#)]
27. Barati, M.R.; Zenkour, A.M. Forced vibration of sinusoidal FG nanobeams resting on hybrid Kerr foundation in hygro-thermal environments. *Mech. Adv. Mater. Struct.* **2018**, *25*, 669–680. [[CrossRef](#)]
28. Zenkour, A.M.; El-Shahrany, H.D. Control of hygrothermal vibration of viscoelastic magnetostrictive laminates resting on Kerr's foundation. *Mech. Based Des. Struct. Mach.* **2021**, *2021*, 1–29. [[CrossRef](#)]
29. Leissa, A.W. The Free vibration of rectangular plates. *J. Sound Vib.* **1973**, *31*, 257–293. [[CrossRef](#)]
30. Zhou, D.; Cheung, Y.K.; Au, F.T.K.; Lo, S.H. Three-dimensional vibration analysis of thick rectangular plates using Chebyshev polynomial and Ritz method. *Int. J. Solids Struct.* **2002**, *39*, 6339–6353. [[CrossRef](#)]
31. Nagino, H.; Mikami, T.; Mizusawa, T. Three-dimensional free vibration analysis of isotropic rectangular plates using the B-spline Ritz method. *J. Sound Vib.* **2008**, *317*, 329–353. [[CrossRef](#)]
32. Liu, F.L.; Liew, K.M. Analysis of vibrating thick rectangular plates with mixed boundary constraints using differential quadrature element method. *J. Sound Vib.* **1999**, *225*, 915–934. [[CrossRef](#)]
33. Hosseini-Hashemi, S.; Fadaee, M.; Taher, H.R.D. Exact solutions for free flexural vibration of Lévy-type rectangular thick plates via third-order shear deformation plate theory. *Appl. Math. Model.* **2011**, *35*, 708–727. [[CrossRef](#)]
34. Shufrin, I.; Eisenberger, M. Stability and vibration of shear deformable plates—First order and higher order analyses. *Int. J. Solids Struct.* **2005**, *42*, 1225–1251. [[CrossRef](#)]
35. Akavci, S.S. An efficient shear deformation theory for free vibration of functionally graded thick rectangular plates on elastic foundation. *Compos. Struct.* **2014**, *108*, 667–676. [[CrossRef](#)]
36. Mantari, J.L.; Granados, E.V.; Hinojosa, M.A.; Guedes Soares, C. Modelling advanced composite plates resting on elastic foundation by using a quasi-3D hybrid type HSDT. *Compos. Struct.* **2014**, *118*, 455–471. [[CrossRef](#)]
37. Matsunaga, H. Vibration and stability of thick plates on elastic foundations. *J. Eng. Mech. ASCE* **2000**, *126*, 27–34. [[CrossRef](#)]
38. Thai, H.T.; Choi, D.H. A refined shear deformation theory for free vibration of functionally graded plates on elastic foundation. *Compos. Part B Eng.* **2012**, *43*, 2335–2347. [[CrossRef](#)]
39. Vel, S.S.; Batra, R.C. Three-dimensional exact solution for the vibration of functionally graded rectangular plate. *J. Sound Vib.* **2004**, *272*, 703–730. [[CrossRef](#)]
40. Neves, A.M.A.; Ferreira, A.J.M.; Carrera, E.; Roque, C.M.C.; Cinefra, M.; Jorge, R.M.N.; Soares, C.M. A quasi-3D sinusoidal shear deformation theory for the static and free vibration analysis of functionally graded plates. *Compos. Part B Eng.* **2012**, *43*, 711–725. [[CrossRef](#)]
41. Neves, A.M.A.; Ferreira, A.J.M.; Carrera, E.; Cinefra, M.; Roque, C.M.C.; Jorge, R.M.N.; Soares, C.M. A quasi-3D hyperbolic shear deformation theory for the static and free vibration analysis of functionally graded plates. *Compos. Struct.* **2012**, *94*, 1814–1825. [[CrossRef](#)]
42. Matsunaga, H. Free vibration and stability of functionally graded plates according to a 2-D higher-order deformation theory. *Compos. Struct.* **2008**, *82*, 499–512. [[CrossRef](#)]
43. Jin, G.; Su, Z.; Shi, S.; Ye, T.; Gao, S. Three-dimensional exact solution for the free vibration of arbitrarily thick functionally graded rectangular plates with general boundary conditions. *Compos. Struct.* **2014**, *108*, 565–577. [[CrossRef](#)]
44. Thai, H.T.; Park, T.; Choi, D.H. An efficient shear deformation theory for vibration of functionally graded plates. *Arch. Appl. Mech.* **2013**, *83*, 137–149. [[CrossRef](#)]
45. Hasani Baferani, A.; Saidi, A.R.; Ehteshami, H. Accurate solution for free vibration analysis of functionally graded thick rectangular plates resting on elastic foundation. *Compos. Struct.* **2011**, *93*, 1842–1853. [[CrossRef](#)]